Supplement of

Contributions of primary sources to submicron organic aerosols in Delhi, India

Sahil Bhandari[1,2], Zainab Arub[3], Gazala Habib[3], Joshua S. Apte[4,5], and Lea Hildebrandt Ruiz[1]

[1]McKetta Department of Chemical Engineering, The University of Texas at Austin, Austin, Texas, USA
[2]Department of Mechanical Engineering, University of British Columbia, Vancouver, Canada
[3]Department of Civil Engineering, Indian Institute of Technology Delhi, New Delhi, India
[4]Department of Civil and Environmental Engineering, UC Berkeley, Berkeley, California, USA
[5]School of Public Health, UC Berkeley, Berkeley, California, USA

Correspondence to: Lea Hildebrandt Ruiz (lhr@che.utexas.edu) and Joshua S. Apte (apte@berkeley.edu)

Note: To refer to PMF runs corresponding to specific time windows in the Supplement, we use the nomenclature "Season" + "Year" + "Period" style in the format "SYYTTTT" (Table S3). For example, W171115 corresponds to the 1100–1500 hours of Winter 2017.

S1 Summary of NR-PM_1 data and key meteorological parameters for Delhi, India

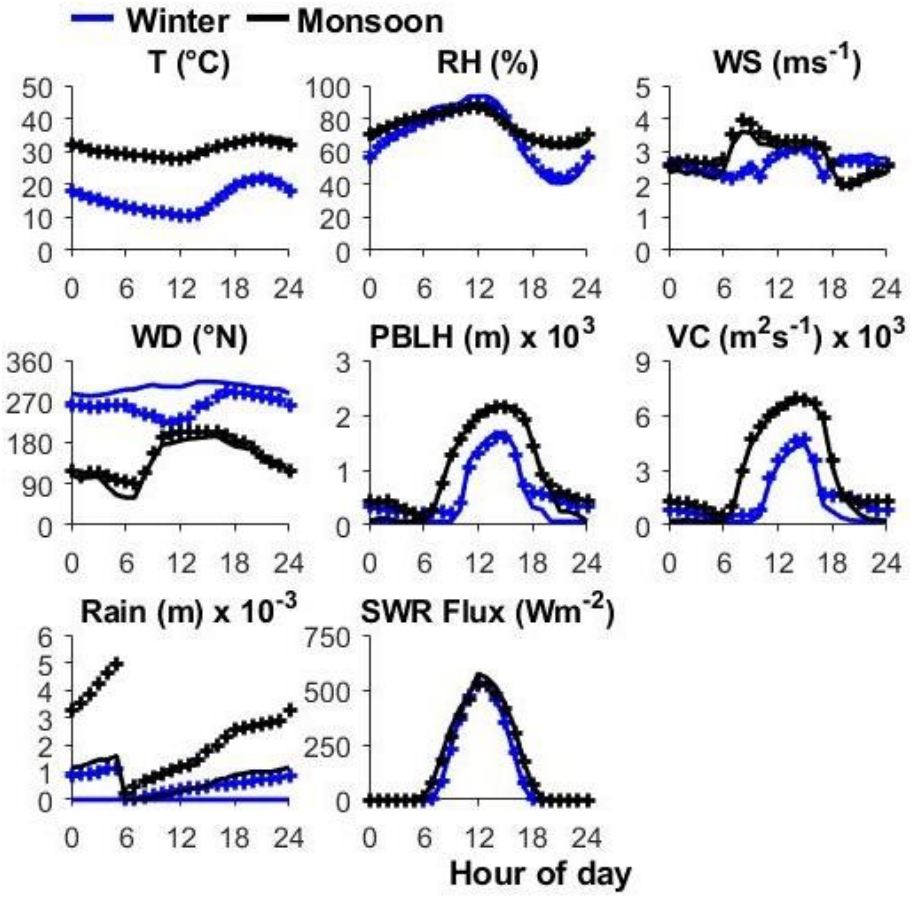

Figure S1 Diurnal profiles of meteorological parameters (temperature, relative humidity, wind speed, wind direction, PBLH, VC, rain, and SWR flux) by season. Mean (+) and median (—) values by season and hour of the day are presented. We retrieved visibility and relative humidity (RH) data from the Indira Gandhi International Airport (IGIA). To obtain mesoscale data for hourly wind speed, direction, temperature (10m above ground level), SWR flux, and planetary boundary layer height (H), we used the NASA meteorological reanalysis dataset (MERRA2). Precipitation data for Delhi was retrieved from the European Centre for Medium-Range Weather Forecasts' reanalysis dataset, ERA-Interim (Gani et al., 2019). The ERA-Interim 12-hour long assimilation windows for precipitation data are from 0600-1800 LT and 1800-0600 LT. The discontinuities in precipitation data occur where windows change. Similar discontinuities have been reported elsewhere as well (ResearchGate, 2021).

Table S1 Seasonal summary of PM_1 species—arithmetic mean (AM) for hourly concentrations (in μg m^{-3}).

	Winter	Monsoon
Org	112	23
NH_4	20	4.6
Chl	23	0.4
NO_3	24	3.6
SO_4	16	10
BC	15	11
NR-	195	41

Table S2 Seasonally averaged meteorological variables in monsoon and winter 2017 (day-D/night-N)

Season	T (K) (D/N)	RH (%) (D/N)	VC (m^2/s)	PBLH (m) (D/N)	WS (m/s) (D/N)	WD (°N) (D/N)
W17	290/286	60/78	707/188	920/340	2.7/2.6	300/300
M17	305/302	71/81	3870/3790	1600/460	3.4/2.5	250/190

S2 Selection of PMF factors and application of factor constraints

Table S3 List of all time periods and PMF factors separated in this study

Period (in hours)	Season	Nomenclature (in main manuscript)	Nomenclature (in the supplement)	Factors separated
1100—1500	Winter	W-11-15	W171115	SFC-OA[a], BBOA, Local OOA, Regional OOA
	Monsoon	M-11-15	M171115	HOA[b], COA[b], Local OOA, Regional OOA
1500—1900	Winter	W-15-19	W171519	HOA, BBOA, Local OOA, Regional OOA
	Monsoon	M-15-19	M171519	HOA, COA, Local OOA, Regional OOA
1900—2300	Winter	W-19-23	W171923	HOA, BBOA, Local OOA, Regional OOA
	Monsoon	M-19-23	M171923	HOA, COA, Local OOA, Regional OOA
2300—0300	Winter	W-23-03	W172303	HOA, BBOA, Local OOA, Regional OOA
	Monsoon	M-23-03	M172303	HOA, COA, Local OOA, Regional OOA
0300—0700	Winter	W-03-07	W170307	HOA[c], BBOA[c], Local OOA, Regional OOA
	Monsoon	M-03-07	M170307	HOA, COA, Local OOA, Regional OOA
0700—1100	Winter	W-07-11	W170711	HOA, BBOA, Local OOA, Regional OOA 1, Regional OOA 2

Period (in hours)	Season	Nomenclature (in main manuscript)	Nomenclature (in the supplement)	Factors separated
	Monsoon	M-07-11	M170711	HOA[b], COA[b], Local OOA, Regional OOA
All day	Winter		W17	HOA, BBOA, Local OOA, Regional OOA
	Monsoon		M17	POA, Local OOA, Regional OOA

[a]For W171115, we were able to separate POA into solid fuel combustion organic aerosol (SFC-OA) and BBOA, not HOA and BBOA. The columns corresponding to HOA and BBOA have entries based on hybrid MLR-PMF-based SFC-OA apportioned to HOA and BBOA

[b]POA separated into HOA and COA using MLR-PMF

[c]POA separated into HOA and BBOA using MLR-PMF

Table S4 List of weak *m/z*s in PMF runs

Period	*m/z*s
W171115	13, 16–18, 24—25, 37—38, 44, 48—49, 62, 66, 75, 76, 80, 88—90, 92, 94, 100—104, 106, 108, 110, 112—114, 116—120
W171519	13, 16—18, 24, 37—38, 44, 49, 88, 90, 92, 94, 100, 102, 112, 114, 116
W171923	13, 16—18, 24—25, 37—38, 44, 49, 104, 116
W172303	13, 15—18, 24, 37—38, 44
W170307	13, 15—18, 24, 37—38, 44
W170711	13, 16—18, 24, 37—38, 44
W17	13, 16—18, 24, 37—38, 44
M171115	13, 16—18, 24, 37, 44, 48—49, 61—62, 66, 72, 75, 80, 86—90, 92, 94, 98, 100—104, 106, 108, 110—114, 116—120
M171519	13, 15—18, 24, 37, 44, 48—49, 61—62, 66, 72, 74—76, 78, 80, 86—90, 92, 94, 96, 98, 100—104, 106, 108, 110—114, 116—120
M171923	13, 15—18, 24, 37—38, 44, 48—49, 62—63, 66, 75—76, 80, 86—90, 94, 100—104, 106, 108, 110, 112—114, 116—118, 120
M172303	13, 16—18, 24—25, 37, 44, 48—49, 61—62, 75—76, 80, 87—90, 94, 100—104, 112—114, 116, 118, 120
M170307	13, 16—18, 24—25, 37—38, 44, 49, 66, 72, 75, 80, 86—90, 94, 100—104, 108, 110, 112—114, 116, 118
M170711	13, 16—18, 24—25, 37—38, 44, 48—49, 62, 66, 72, 75—76, 80, 87—90, 92, 94, 100—104, 106, 108, 110—114, 116—120
M17	13, 16—18, 24, 37, 44, 48—49, 62, 66, 72, 75, 76, 80, 86—90, 94, 100—104, 108, 110, 112—114, 116, 118, 120

Table S5 Steps for solution identification for specific EPA PMF runs

Period	Solution identification
W171115	Residual analysis suggested 4–6 factor solutions. Factor swaps occurring in 5 and 6 factor solutions. Application of constraints at 5 and 6 factor solutions resulted in unreasonable MS or weak time series correlations. Base 4 factor solution fails BS test. Rotating the solution to FPEAK of 1 led to BS test resolution.
W171519	Residual analysis suggested 4–6 factor solutions. Solutions with 5 or more factors generate two or more factors with no time series correlations. Base run for 4 factor solution passes BS and DISP but shows factor swaps in BS-DISP occurring between multiple factors. Application of constraints on regional OOA and BBOA factors led to BS-DISP test resolution.
W171923	Residual analysis suggested 3–5 factor solutions. Base runs of 5 factor solutions fail at BS and base runs of 4 factor solutions pass BS but fail DISP. 3 factor solutions pass the three tests but with many swaps. High swaps at low factor number suggested applications of constraints necessary. Solutions with 5 or more factors show factor swaps at three or more factors despite application of constraints. Base run for 4 factor solution passes BS and DISP but shows large number of factor swaps in BS-DISP occurring between HOA and BBOA. Application of constraints on BBOA led to BS-DISP test resolution and improvements in BS and DISP results.
W170307	Residual analysis suggested 5–7 factor solutions. However, 5 factor and higher factor solutions have mismatched MS and TS correlations. 5 factor base run passes BS and DISP but fails BS-DISP at multiple factors, despite application of rotations or constraints. Base runs of 4 factor solution passes BS on rotation but shows factors swaps across all four factors in the BS-DISP test. Constraining factors did not solve the problem. Base run of the 3-factor solution passed all three tests sufficiently.
W172303	Residual analysis suggested 6–8 factor solutions. Attempted rotations and constraints for solutions with 6 or more factors but failed BS and DISP repeatedly. Base runs of 5 factor solutions fail DISP and show factor swaps at two or more factors, despite the application of rotations and constraints. Base runs of 4 factor solution fail BS at a semi-volatile oxidized OA factor, that shows mixing with HOA and BBOA factors. Constraining primary factors did not solve the problem. Rotations of the 4-factor solution allowed passing of the BS test but failed DISP. Finally, constraints based on the SVOOA reference profile were applied on the semi-volatile oxidized OA factor. Application of these constraints led to passing of all three tests.
W170711	Residual analysis suggested 5–7 factor solutions. However, 6 factor and higher factor solutions have mismatched MS and TS correlations. Base run at 5 factor solution passes BS and DISP but fails BS-DISP at multiple factors, despite application of rotations or constraints. Constraining factor 2 as HOA led to BS-DISP test resolution.
W17	Residual analysis suggested 4–6 factor solutions. 5 and 6 factor solutions resulted in unreasonable MS or weak time series correlations. 4 factor solution fails BS-DISP test and shows factor swaps of BBOA, HOA, and local OOA factors. Constraining BBOA led to BS-DISP test resolution as well as improves BS mapping.

Table S5 (continued)

Period	Solution identification
M171115	Residual analysis suggested 3–5 factor solutions. 4 and 5 factor solution resulted in unreasonable MS or weak time series correlations. 3 factor solution base run passes all tests.
M171519	Residual analysis suggested 3–5 factor solutions. 5 factor solution resulted in two pairs of factors with identical correlations, suggesting factors splitting. Base run from the 4 factor solution shows mixing of 2 factors, suggests mixing of HOA, COA. Factor 2 MS resembles COA MS. Solution with factor 2 constrained as COA passes all tests.
M171923	Residual analysis suggested 3–5 factor solutions. 5 factor solutions resulted in two factors with no time series correlations. Base run at 4 factor solution passes BS, DISP and BS-DISP tests.
M172303	Residual analysis suggested 3–5 factor solutions. 5 factor solutions resulted in two factors with no time series correlations. 4 factor solution passes DISP and BS-DISP tests but fails BS test. Rotating solution to FPEAK 15 led to the necessary improvement in BS mapping.
M170307	Residual analysis suggested 3–6 factor solutions. 5 or more factor solutions resulted in factors with mismatched mass spectral and time series correlations. 4 factor solution shows evidence of factor mixing of regional OOA and local OOA in BS and DISP. Base run factor 2 resembles COA MS. Constraining presence of COA in the solution resulted in solution that passes BS, DISP, and BS-DISP tests.
M170711	Residual analysis suggested 3–6 factor solutions. 5 or more factor solutions resulted in factors with mismatched mass spectral and time series correlations. 4 factor solutions gave identical correlations at two factors, suggesting factor splitting. Constraining presence of HOA and COA in the solution resulted in mismatched mass spectral and time series correlations. Base run at 3 factor solution passes BS, DISP, and BS-DISP tests.
M17	Residual analysis suggested 3–5 factor solutions. Solutions 4 factors and above gave identical TS correlations at multiple factors.

Table S6 Details of number of factors, seed, constraints, and rotations applied in EPA PMF

Period	Solution Identification
W171115	4 factor solution at seed 83 was rotated to FPEAK 1
W171519	4 factor solution at seed 51 was constrained with regional OOA presence at factor 3 and BBOA presence at factor 4
W171923	4 factor solution at seed 27 was constrained with BBOA presence at factor 1
W172303	4 factor solution at seed 6 was constrained with SVOOA presence at factor 3
W170307	3 factor solution at seed 27 with no constraints or rotations applied
W170711	5 factor solution at seed 44 was constrained with HOA presence at factor 2

Period	Solution Identification
W17	4 factor solution at seed 5 was constrained with BBOA presence at factor 1
M171115	3 factor solution at seed 76 with no constraints or rotations applied
M171519	4 factor solution at seed 67 was constrained with COA presence at factor 2
M171923	4 factor solution at seed 1 with no constraints or rotations applied
M172303	4 factor solution at seed 54 was rotated to FPEAK 15
M170307	4 factor solution at seed 44 was constrained with COA presence at factor 2
M170711	3 factor solution at seed 99 with no constraints or rotations applied
M17	3 factor solution at seed 83 with no constraints or rotations applied

Table S7 Details of block size calculations for all PMF runs

Period	Mean block size	Median block size	Block size for total organics	Percentile calculations		Used block size
				Percentile	Block size	
W171115	36	36	42	90	43	43
W171519	36	36	41	75	42	42
W171923	50	50	51	90	51	51
W172303	53	53	53	100	54	54
W170307	54	55	55	70	55	56
W170711	44	45	46	85	47	47
M171923	98	100	100	80	101	101
M171115	94	94	97	90	98	98
M172303	98	99	100	75	100	100
M170307	99	101	102	95	102	102
M170711	99	99	100	95	101	101
M171519	95	95	97	85	97	97
M17	296	296	309	75	310	310
W17	160	160	161	90	162	162

Table S8 BS mapping results (reported in terms of BS mapping observed in period)

Period	Factors separated in EPA PMF	BS mapping (out of 100)
W171115	SFC-OA, BBOA, Local OOA, Regional OOA	100, 92, 100, 95
W171519	HOA, BBOA, Local OOA, Regional OOA	97, 97, 97, 94
W171923	HOA, BBOA, Local OOA, Regional OOA	100, 100, 99, 100
W172303	HOA, BBOA, Local OOA, Regional OOA	100, 99, 97, 100
W170307	POA, Local OOA, Regional OOA	100, 85, 100
W170711	HOA, BBOA, Local OOA, Regional OOA 1, Regional OOA 2	99, 94, 88, 99, 81
W17	HOA, BBOA, Local OOA, Regional OOA	100, 100, 100, 100
M171115	POA, Local OOA, Regional OOA	95, 77, 100
M171519	HOA, COA, Local OOA, Regional OOA	99, 95, 99, 99
M171923	HOA, COA, Local OOA, Regional OOA	100, 100, 83, 89
M172303	HOA, COA, Local OOA, Regional OOA	100, 100, 96, 99
M170307	HOA, COA, Local OOA, Regional OOA	90, 90, 90, 90
M170711	POA, Local OOA, Regional OOA	99, 92, 100
M17	POA, Local OOA, Regional OOA	NA[a]

[a]Test terminated due to large computational size of data

Table S9 DISP swap performance results for lowest dQ-max

Period	Solution identification	DISP swaps
W171115	SFC-OA, BBOA, Local OOA, Regional OOA	0, 0, 0, 0
W171519	HOA, BBOA, Local OOA, Regional OOA	0, 0, 0, 0
W171923	HOA, BBOA, Local OOA, Regional OOA	0, 0, 0, 0
W172303	HOA, BBOA, Local OOA, Regional OOA	0, 0, 0, 0
W170307	POA, Local OOA, Regional OOA	0, 0, 0
W170711	HOA, BBOA, Local OOA, Regional OOA 1, Regional OOA 2	0, 0, 0, 0, 0
W17	HOA, BBOA, Local OOA, Regional OOA	0, 0, 0, 0
M171115	POA, Local OOA, Regional OOA	0, 0, 0
M171519	HOA, COA, Local OOA, Regional OOA	0, 0, 0, 0
M171923	HOA, COA, Local OOA, Regional OOA	0, 0, 0, 0
M172303	HOA, COA, Local OOA, Regional OOA	0, 0, 0, 0
M170307	HOA, COA, Local OOA, Regional OOA	0, 0, 0, 0
M170711	POA, Local OOA, Regional OOA	0, 0, 0
M17	POA, Local OOA, Regional OOA	0, 0, 0, 0

Table S10 BS-DISP swap performance results for lowest dQ-max

Period	Factors separated in EPA PMF	Accepted cases	BS-DISP swaps
W171115	SFC-OA, BBOA, Local OOA, Regional OOA	82	2, 1, 0, 3
W171519	HOA, BBOA, Local OOA, Regional OOA	37	0, 0, 0, 0
W171923	HOA, BBOA, Local OOA, Regional OOA	47	4, 4, 1, 1
W172303	HOA, BBOA, Local OOA, Regional OOA	NA[a]	0, 0, 0, 0
W170307	POA, Local OOA, Regional OOA	85	3, 3, 2
W170711	HOA, BBOA, Local OOA, Regional OOA 1, Regional OOA 2	NA[a]	0, 0, 0, 0
W17	HOA, BBOA, Local OOA, Regional OOA	83	11, 7, 4, 0
M171115	POA, Local OOA, Regional OOA	98	0, 0, 0
M171519	HOA, COA, Local OOA, Regional OOA	87	0, 0, 0, 0
M171923	HOA, COA, Local OOA, Regional OOA	94	0, 0, 0, 0
M172303	HOA, COA, Local OOA, Regional OOA	93	1, 1, 0, 0
M170307	HOA, COA, Local OOA, Regional OOA	54	0, 0, 0, 0
M170711	POA, Local OOA, Regional OOA	95	0, 0, 0
M17	POA, Local OOA, Regional OOA	NA[b]	NA

[a]Test terminated prematurely due to unknown cause [b]Test terminated due to large computational size of data

Table S11 Average fractional contributions of time-of-day PMF factors for winter 2017 (in %)

Period	HOA	BBOA	COA	POA	OOA
W171115[a]	6.4	25	0	31	69
W171519	22	14	0	36	64
W171923	20	29	0	50	50
W172303	18	21	0	40	60
W170307[b]	14	9	0	23	77
W170711	13	14	0	27	73
W17 Avg.	16	19	0	34	66

[a]For W171115, we were able to separate POA into SFC-OA and BBOA, not HOA and BBOA. The columns corresponding to HOA and BBOA have entries based on hybrid MLR-PMF-based SFC-OA apportioned to HOA and BBOA

[b]For W170307, columns corresponding to HOA and BBOA have entries based on hybrid MLR-PMF-based POA apportioned to HOA and BBOA

Table S12 Average fractional contributions of time-of-day PMF factors for monsoon 2017 (in %)

Period	HOA	BBOA	COA	POA	OOA
M171115[a]	7	1[b]	13	21	79
M171519	21	0	8	28	72
M171923	17	0	22	39	61
M172303	21	0	14	36	64
M170307	17	0	15	32	68
M170711[a]	2	0	16	20	82
M17 Avg.	14	0	15	29	71

[a]Hybrid MLR-PMF-based results for M171115 and M170711

[b]BBOA mass below organic detection limit in the ACSM (Ng et al., 2011b) (see Table 2)

Table S13 Detailed comparisons of seasonal and time-of-day PMF factor concentrations for time-of-day periods in winter 2017 (in µg m^{-3}).

Period	Time-of-day PMF			Seasonal PMF		
	POA	OOA	Total	POA (HOA, BBOA)	OOA	Total
W171115	23	47	70	13 (3.5, 9.7)	55	69
W171519	23	35	58	16 (8.0, 7.9)	41	57
W171923	76	66	142	87 (48, 40)	55	142
W172303	72	71	143	86 (49, 37)	57	143
W170307	36	80	117	57 (29, 28)	60	117
W170711	36	83	119	51 (22, 29)	69	120

Table S14 Detailed comparisons of seasonal and time-of-day PMF factor concentrations for time-of-day periods in monsoon 2017 (in µg m^{-3}).

Period	Time-of-day PMF			Seasonal PMF		
	POA	OOA	Total	POA	OOA	Total
M171115	4.0	17	21	2.5	19	21
M171519	5.1	13	18	2.7	15	17
M171923	12	18	30	9.7	20	30
M172303	12	18	30	8.7	21	30
M170307	7.9	15	23	4.6	18	23
M170711	4.4	20	24	3.8	20	24

Table S15 Comparison of UMR-MS ion signals at m/z 29, m/z 43, m/z 44, m/z 55, m/z 57, m/z 60, and m/z 73 of HOA from winter 2017 time-of-day PMF and seasonal PMF with the reference HOA MS profile reported in the literature (Ng et al., 2011a)

m/z	W171115	W171519	W171923	W172303	W170307	W170711	W17	Ref. HOA	SD (Ref. HOA)
29	4.0E-02	4.7E-02	2.5E-02	3.6E-02	3.8E-02	3.4E-02	2.4E-02	3.8E-02	2.3E-02
41	8.3E-02	6.4E-02	6.7E-02	6.3E-02	8.0E-02	7.1E-02	6.2E-02	8.0E-02	1.7E-02
43	1.1E-01	1.0E-01	9.5E-02	9.6E-02	1.1E-01	9.4E-02	9.6E-02	1.1E-01	2.7E-02
44	1.6E-02	6.5E-02	3.1E-02	3.5E-02	1.5E-02	1.4E-02	4.3E-02	1.5E-02	1.2E-02
55	9.3E-02	6.3E-02	7.7E-02	7.1E-02	8.9E-02	7.9E-02	6.8E-02	8.9E-02	1.8E-02
57	8.8E-02	6.2E-02	7.3E-02	6.9E-02	8.5E-02	7.5E-02	6.5E-02	8.4E-02	3.5E-02
60	2.4E-03	0.0E+00	8.1E-03	1.4E-02	2.3E-03	2.0E-02	1.1E-02	2.3E-03	2.0E-03
73	2.5E-03	1.4E-03	7.2E-03	8.8E-03	2.4E-03	1.2E-02	7.3E-03	2.4E-03	1.8E-03

Table S16 Comparison of UMR-MS ion signals at m/z 29, m/z 43, m/z 44, m/z 55, m/z 57, m/z 60, and m/z 73 of BBOA from winter 2017 time-of-day PMF with the reference BBOA MS profile reported in the literature (Ng et al., 2011a)

m/z	W171115	W171519	W171923	W172303	W170307	W170711	W17	Ref. BBOA	SD (Ref. BBOA)
29	1.2E-01	8.6E-02	1.0E-01	1.2E-01	1.5E-01	8.0E-02	1.6E-01	6.7E-02	1.6E-02
41	4.3E-02	5.0E-02	5.0E-02	4.7E-02	2.8E-02	4.7E-02	4.5E-02	3.7E-02	1.5E-03
43	9.1E-02	7.9E-02	7.4E-02	7.6E-02	6.5E-02	8.8E-02	7.1E-02	6.2E-02	1.2E-03
44	5.6E-02	3.7E-02	3.4E-02	3.8E-02	0.0E+00	0.0E+00	1.1E-03	2.9E-02	7.9E-04
55	3.2E-02	4.6E-02	4.3E-02	4.7E-02	2.7E-02	4.2E-02	4.2E-02	3.6E-02	5.9E-03
57	2.5E-02	3.6E-02	3.4E-02	5.0E-02	4.4E-02	5.0E-02	4.3E-02	2.8E-02	7.4E-03
60	1.8E-02	2.7E-02	2.5E-02	3.0E-02	5.7E-02	2.3E-02	3.5E-02	2.1E-02	4.4E-03
73	1.1E-02	1.6E-02	1.5E-02	1.6E-02	2.6E-02	1.5E-02	2.0E-02	1.2E-02	4.5E-03

Table S17 Comparison of UMR-MS ion signals at m/z 29, m/z 43, m/z 44, m/z 55, m/z 57, m/z 60, and m/z 73 of HOA from monsoon 2017 time-of-day PMF with the reference HOA MS profile reported in the literature (Ng et al., 2011a)

m/z	M171115	M171519	M171923	M172303	M170307	M170711	Ref. HOA	SD (Ref. HOA)
29	3.9E-02	5.4E-02	6.2E-02	7.2E-02	7.0E-02	4.0E-02	3.8E-02	2.3E-02
41	8.3E-02	8.9E-02	8.2E-02	8.7E-02	9.1E-02	8.4E-02	8.0E-02	1.7E-02
43	1.1E-01	1.2E-01	1.5E-01	1.1E-01	1.1E-01	1.1E-01	1.1E-01	2.7E-02
44	1.6E-02	0.0E+00	1.4E-02	0.0E+00	0.0E+00	1.6E-02	1.5E-02	1.2E-02

55	9.2E-02	7.3E-02	7.5E-02	8.5E-02	7.3E-02	9.3E-02	8.9E-02	1.8E-02
57	8.7E-02	6.3E-02	9.1E-02	7.5E-02	6.7E-02	8.8E-02	8.4E-02	3.5E-02
60	2.4E-03	5.2E-03	5.1E-04	4.8E-03	3.4E-03	2.4E-03	2.3E-03	2.0E-03
73	2.5E-03	3.7E-03	4.9E-04	4.3E-03	3.8E-03	2.6E-03	2.4E-03	1.8E-03

Table S18 Comparison of UMR-MS ion signals at m/z 29, m/z 43, m/z 44, m/z 55, m/z 57, m/z 60, and m/z 73 of COA from monsoon 2017 time-of-day PMF with the reference COA MS profile reported in the literature (Hu et al., 2016)

m/z	M171115	M171519	M171923	M172303	M170307	M170711	Ref. COA
29	1.5E-01	4.8E-02	5.1E-02	0.0E+00	5.5E-02	0.0E+00	5.5E-02
41	7.4E-02	6.6E-02	9.4E-02	1.0E-01	7.6E-02	8.9E-02	8.7E-02
43	2.3E-02	4.0E-02	2.4E-02	5.7E-02	4.6E-02	1.2E-01	6.3E-02
44	6.9E-02	1.4E-02	0.0E+00	9.2E-03	3.6E-02	7.4E-03	2.2E-02
55	4.9E-02	5.6E-02	7.9E-02	7.3E-02	6.5E-02	7.1E-02	8.1E-02
57	2.6E-02	3.0E-02	4.0E-02	4.4E-02	3.5E-02	4.7E-02	3.1E-02
60	5.0E-03	3.9E-03	9.2E-03	4.7E-03	6.1E-03	7.5E-03	4.4E-03
73	3.5E-03	4.7E-03	6.7E-03	4.1E-03	4.0E-03	5.9E-03	4.1E-03

90

Table S19 UMR-MS ion signals at m/zs 29, 43, 44, 55, 57, 60, and 73 of POA from winter 2017 time-of-day PMF

m/z	W171115	W171519	W171923	W172303	W170307	W170711
29	1.0E-01	6.5E-02	6.9E-02	7.8E-02	7.8E-02	5.6E-02
41	5.1E-02	5.8E-02	5.8E-02	5.5E-02	5.9E-02	6.0E-02
43	9.5E-02	9.1E-02	8.3E-02	8.6E-02	8.8E-02	9.1E-02
44	4.8E-02	5.2E-02	3.3E-02	3.7E-02	8.5E-04	7.1E-03
55	4.5E-02	5.5E-02	5.7E-02	6.0E-02	6.4E-02	6.1E-02
57	3.8E-02	5.0E-02	5.0E-02	6.0E-02	6.7E-02	6.3E-02
60	1.5E-02	1.2E-02	1.8E-02	2.2E-02	2.3E-02	2.1E-02
73	8.9E-03	7.9E-03	1.1E-02	1.2E-02	1.3E-02	1.3E-02

Table S20 UMR-MS ion signals at m/zs 29, 43, 44, 55, 57, 60, and 73 of POA from winter 2017 seasonal PMF

m/z	W171115	W171519	W171923	W172303	W170307	W170711
29	1.2E-01	8.1E-02	8.6E-02	7.9E-02	8.3E-02	9.5E-02
41	5.0E-02	5.5E-02	5.4E-02	5.5E-02	5.5E-02	5.3E-02
43	7.9E-02	8.6E-02	8.5E-02	8.7E-02	8.6E-02	8.4E-02
44	1.4E-02	2.6E-02	2.5E-02	2.7E-02	2.6E-02	2.2E-02
55	5.0E-02	5.7E-02	5.7E-02	5.8E-02	5.7E-02	5.5E-02
57	5.0E-02	5.6E-02	5.5E-02	5.7E-02	5.6E-02	5.4E-02
60	2.7E-02	2.1E-02	2.1E-02	2.0E-02	2.1E-02	2.3E-02
73	1.6E-02	1.2E-02	1.3E-02	1.2E-02	1.3E-02	1.4E-02

95

Table S21 UMR-MS ion signals at m/zs 29, 43, 44, 55, 57, 60, and 73 of POA from monsoon 2017 time-of-day PMF

m/z	M171115	M171519	M171923	M172303	M170307	M170711
29	1.1E-01	5.2E-02	5.7E-02	4.9E-02	6.4E-02	0.0E+00
41	7.2E-02	8.3E-02	8.8E-02	9.1E-02	8.5E-02	8.6E-02
43	5.0E-02	9.6E-02	8.9E-02	9.4E-02	8.7E-02	1.2E-01
44	4.9E-02	3.5E-03	7.4E-03	2.9E-03	1.4E-02	8.1E-03
55	6.0E-02	6.9E-02	7.7E-02	8.1E-02	7.0E-02	7.2E-02
57	4.4E-02	5.5E-02	6.6E-02	6.5E-02	5.4E-02	5.0E-02
60	4.7E-03	4.9E-03	4.7E-03	4.8E-03	4.4E-03	6.9E-03
73	3.4E-03	4.0E-03	3.5E-03	4.2E-03	3.9E-03	5.4E-03

Table S22 UMR-MS ion signals at m/zs 29, 43, 44, 55, 57, 60, and 73 of POA from monsoon 2017 seasonal PMF

m/z	M171115	M171519	M171923	M172303	M170307	M170711
29	5.4E-02	5.4E-02	5.4E-02	5.4E-02	5.4E-02	5.4E-02
41	9.0E-02	9.0E-02	9.0E-02	9.0E-02	9.0E-02	9.0E-02
43	1.1E-01	1.1E-01	1.1E-01	1.1E-01	1.1E-01	1.1E-01
44	0.0E+00	0.0E+00	0.0E+00	0.0E+00	0.0E+00	0.0E+00
55	8.0E-02	8.0E-02	8.0E-02	8.0E-02	8.0E-02	8.0E-02
57	6.7E-02	6.7E-02	6.7E-02	6.7E-02	6.7E-02	6.7E-02
60	5.2E-03	5.2E-03	5.2E-03	5.2E-03	5.2E-03	5.2E-03
73	4.2E-03	4.2E-03	4.2E-03	4.2E-03	4.2E-03	4.2E-03

Table S23 Comparison of UMR-MS ion signals at m/z 29, m/z 43, m/z 44, m/z 55, m/z 57, m/z 60, and m/z 73 of OOA from winter 2017 time-of-day PMF with the reference OOA MS profile reported in the literature (Ng et al., 2011a)

m/z	W171115	W171519	W171923	W172303	W170307	W170711	Ref. OOA	SD (Ref. OOA)
29	7.0E-02	8.5E-02	8.9E-02	7.5E-02	8.0E-02	9.8E-02	5.3E-02	2.6E-02
41	2.8E-02	2.5E-02	3.6E-02	3.8E-02	3.8E-02	3.5E-02	3.6E-02	9.4E-03
43	7.5E-02	7.2E-02	8.2E-02	8.1E-02	8.2E-02	8.0E-02	8.0E-02	2.2E-02
44	1.8E-01	1.8E-01	1.2E-01	1.2E-01	1.3E-01	1.3E-01	1.4E-01	3.3E-02
55	2.5E-02	2.1E-02	3.3E-02	3.1E-02	3.1E-02	3.0E-02	2.7E-02	9.0E-03
57	1.3E-02	7.4E-03	2.5E-02	2.0E-02	2.1E-02	1.8E-02	9.6E-03	7.6E-03
60	3.8E-03	6.3E-03	1.2E-02	6.5E-03	8.3E-03	8.1E-03	5.5E-03	3.4E-03
73	4.2E-03	5.1E-03	7.8E-03	6.3E-03	6.3E-03	6.2E-03	3.6E-03	1.1E-03

Table S24 Comparison of UMR-MS ion signals at m/z 29, m/z 43, m/z 44, m/z 55, m/z 57, m/z 60, and m/z 73 of OOA from winter 2017 seasonal PMF with the reference OOA MS profile reported in the literature (Ng et al., 2011a).

m/z	W171115	W171519	W171923	W172303	W170307	W170711	Ref. OOA	SD (Ref. OOA)
29	7.2E-02	7.1E-02	6.7E-02	6.7E-02	6.8E-02	6.9E-02	5.3E-02	2.6E-02
41	3.4E-02	3.4E-02	3.5E-02	3.5E-02	3.5E-02	3.4E-02	3.6E-02	9.4E-03
43	8.2E-02	8.2E-02	8.0E-02	8.0E-02	8.1E-02	8.1E-02	8.0E-02	2.2E-02
44	1.6E-01	1.6E-01	1.5E-01	1.5E-01	1.5E-01	1.6E-01	1.4E-01	3.3E-02
55	2.8E-02	2.8E-02	2.8E-02	2.8E-02	2.8E-02	2.8E-02	2.7E-02	9.0E-03
57	1.4E-02	1.4E-02	1.5E-02	1.5E-02	1.5E-02	1.5E-02	9.6E-03	7.6E-03
60	2.4E-03	2.5E-03	4.2E-03	4.0E-03	3.9E-03	3.3E-03	5.5E-03	3.4E-03
73	3.1E-03	3.2E-03	4.3E-03	4.2E-03	4.1E-03	3.7E-03	3.6E-03	1.1E-03

Table S25 Comparison of UMR-MS ion signals at m/z 29, m/z 43, m/z 44, m/z 55, m/z 57, m/z 60, and m/z 73 of OOA from monsoon 2017 time-of-day PMF with the reference OOA MS profile reported in the literature (Ng et al., 2011a).

m/z	M171115	M171519	M171923	M172303	M170307	M170711	Ref. OOA	SD (Ref. OOA)
29	9.0E-02	9.8E-02	9.4E-02	1.0E-01	8.9E-02	1.1E-01	5.3E-02	2.6E-02
41	3.4E-02	2.7E-02	3.5E-02	2.9E-02	3.0E-02	3.6E-02	3.6E-02	9.4E-03
43	8.2E-02	6.6E-02	7.1E-02	7.1E-02	7.4E-02	6.6E-02	8.0E-02	2.2E-02
44	1.5E-01	1.8E-01	1.5E-01	1.6E-01	1.6E-01	1.4E-01	1.4E-01	3.3E-02
55	2.6E-02	2.0E-02	2.5E-02	1.9E-02	2.1E-02	2.8E-02	2.7E-02	9.0E-03
57	1.3E-02	7.0E-03	1.0E-02	7.7E-03	1.1E-02	1.5E-02	9.6E-03	7.6E-03
60	3.6E-03	3.2E-03	5.2E-03	5.2E-03	5.0E-03	4.5E-03	5.5E-03	3.4E-03
73	3.2E-03	2.8E-03	3.9E-03	3.7E-03	3.6E-03	3.3E-03	3.6E-03	1.1E-03

Table S26 Comparison of UMR-MS ion signals at m/z 29, m/z 43, m/z 44, m/z 55, m/z 57, m/z 60, and m/z 73 of OOA from monsoon 2017 seasonal PMF with the reference OOA MS profile reported in the literature (Ng et al., 2011a).

m/z	M171115	M171519	M171923	M172303	M170307	M170711	Ref. OOA	SD (Ref. OOA)
29	9.4E-02	9.4E-02	9.0E-02	9.0E-02	9.1E-02	9.2E-02	5.3E-02	2.6E-02
41	3.5E-02	3.6E-02	4.0E-02	3.9E-02	3.8E-02	3.7E-02	3.6E-02	9.4E-03
43	7.2E-02	7.1E-02	6.4E-02	6.6E-02	6.7E-02	6.9E-02	8.0E-02	2.2E-02
44	1.5E-01	1.5E-01	1.4E-01	1.4E-01	1.4E-01	1.4E-01	1.4E-01	3.3E-02
55	2.5E-02	2.6E-02	2.9E-02	2.9E-02	2.8E-02	2.7E-02	2.7E-02	9.0E-03
57	1.2E-02	1.3E-02	1.5E-02	1.4E-02	1.4E-02	1.3E-02	9.6E-03	7.6E-03
60	4.2E-03	4.3E-03	4.7E-03	4.6E-03	4.5E-03	4.4E-03	5.5E-03	3.4E-03
73	3.3E-03	3.4E-03	3.6E-03	3.5E-03	3.5E-03	3.4E-03	3.6E-03	1.1E-03

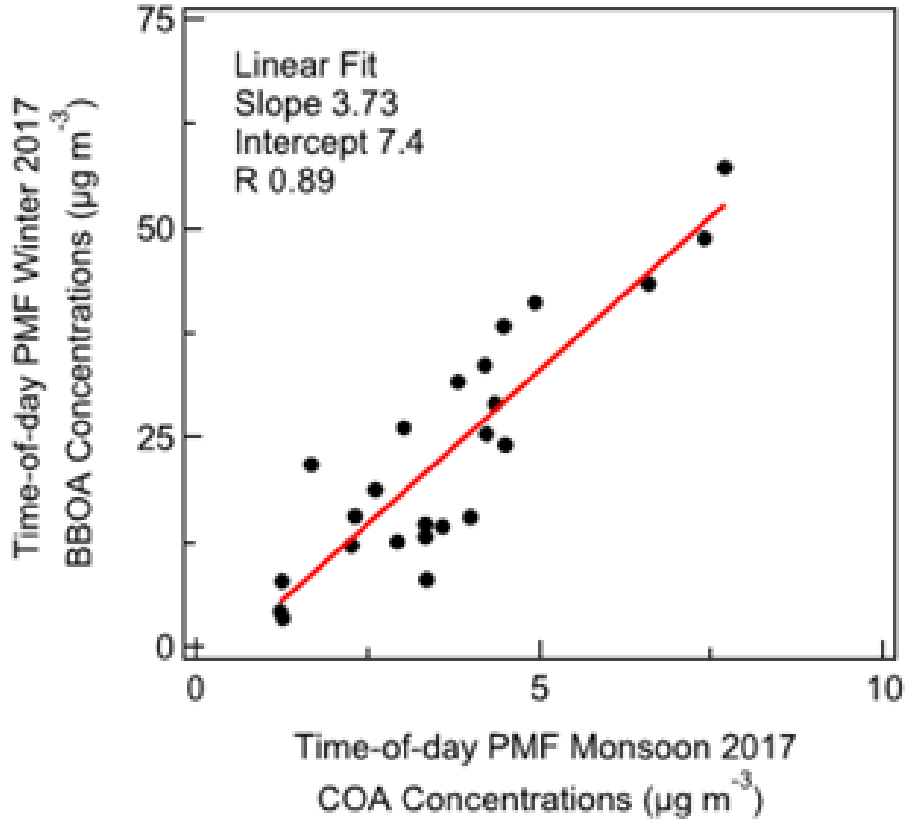

Figure S2 Comparison of seasonally representative diurnal mean concentrations of BBOA (winter 2017) and COA (monsoon 2017) (in µg m^{-3}). Time-of-day PMF BBOA from winter 2017 and COA from monsoon 2017 are strongly correlated, suggesting similar sources of the two PMF factors.

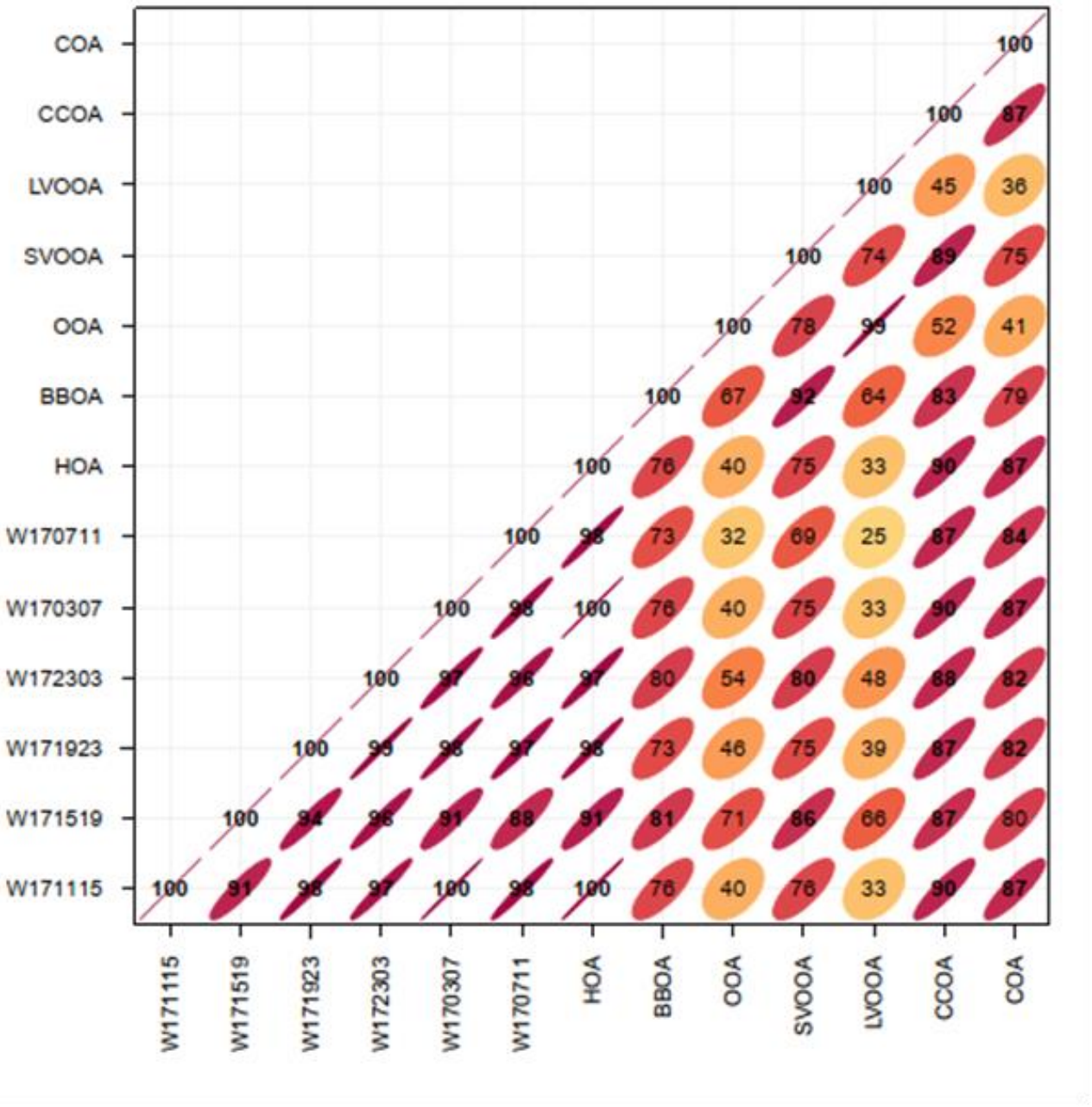

Figure S3 shows the mass spectral comparison of the time-of-day PMF HOA MS profiles for winter 2017. Time-of-day PMF HOA MS is strongly correlated to reference HOA MS profile.

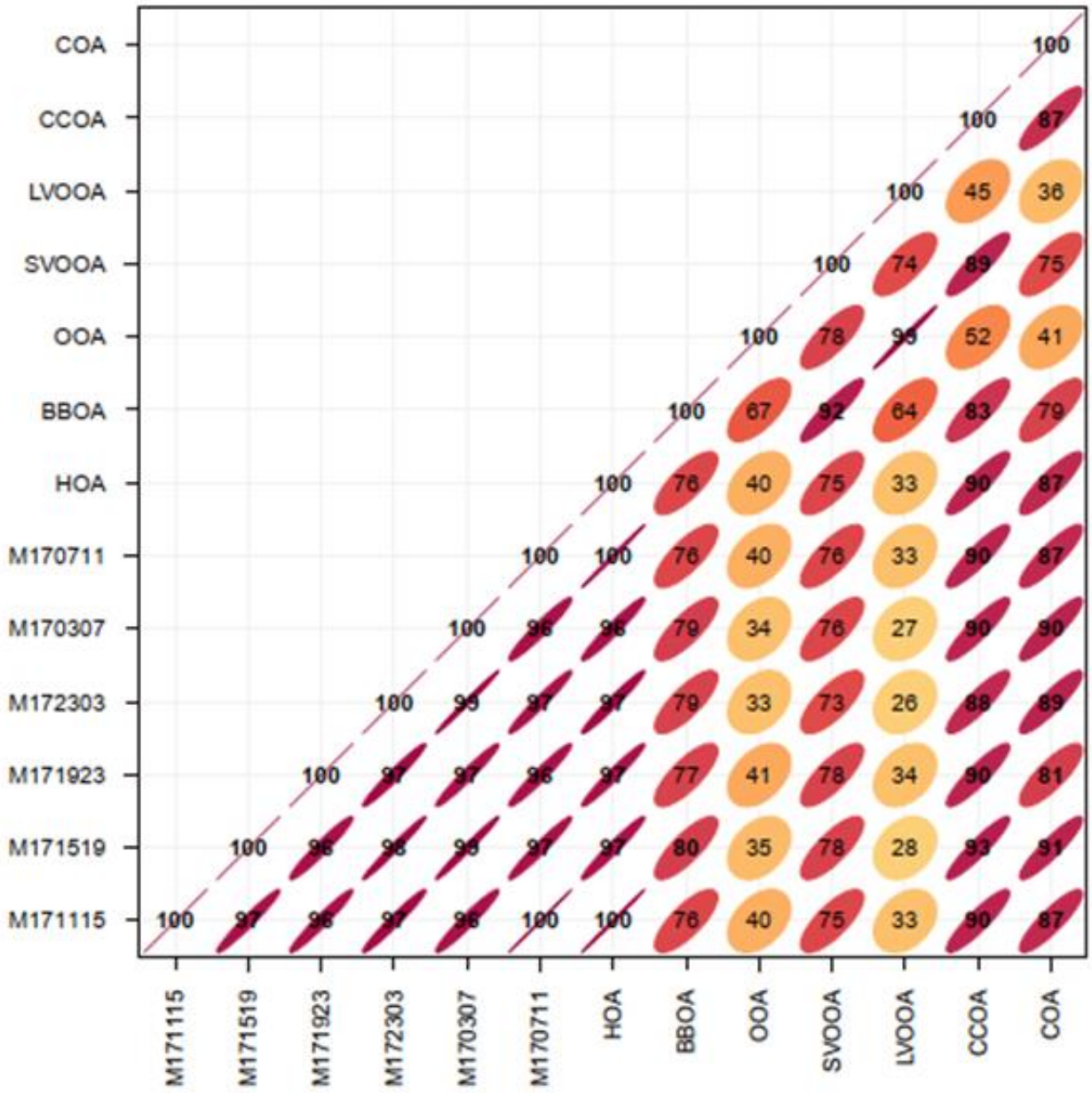

Figure S4 shows the mass spectral comparison of the time-of-day PMF HOA MS profiles for monsoon 2017. Time-of-day PMF HOA MS is strongly correlated to reference HOA MS profile.

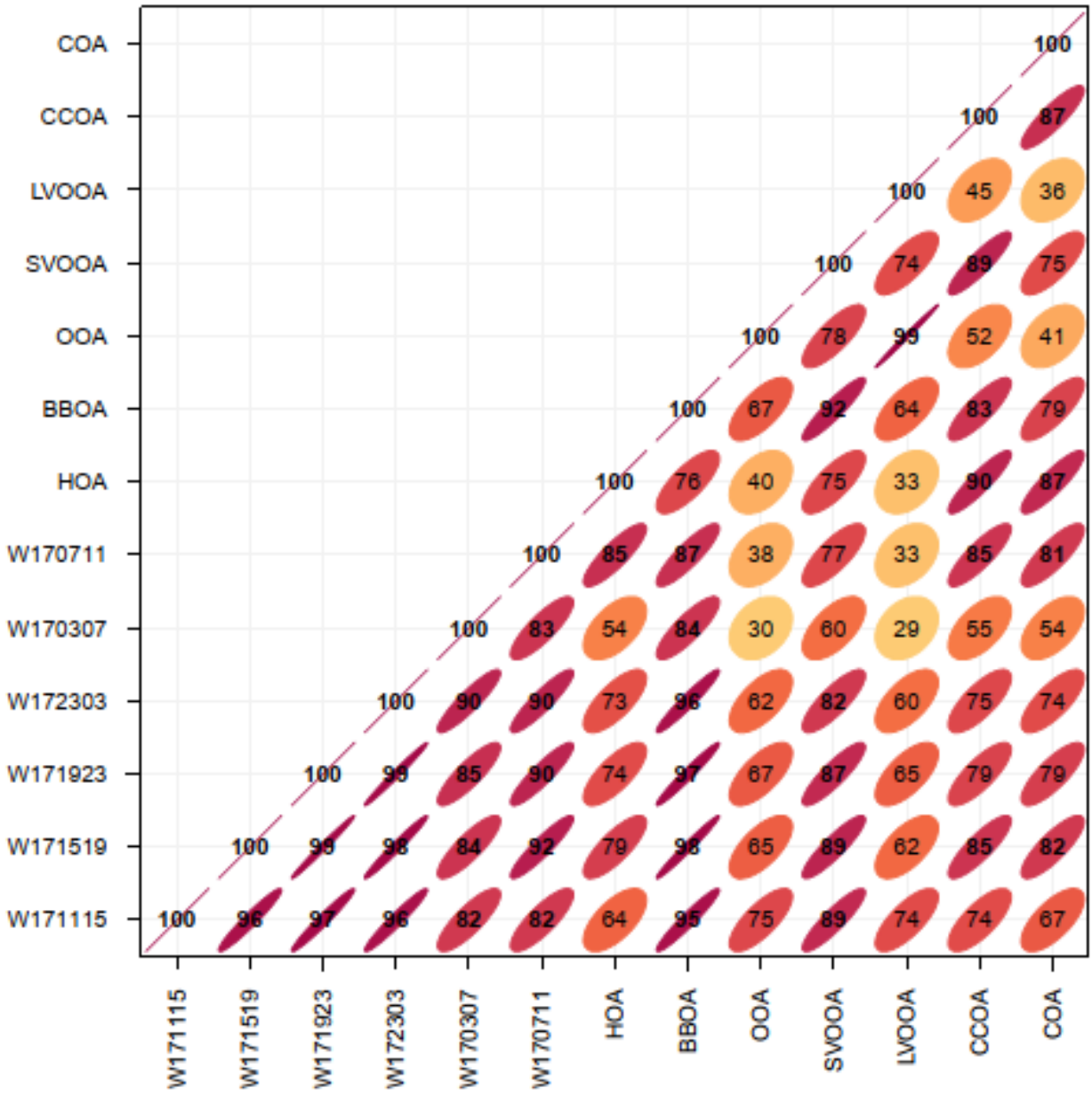

125 **Figure S5 shows the mass spectral comparison of the time-of-day PMF BBOA MS profiles for winter 2017. Time-of-day PMF BBOA MS is strongly correlated to reference BBOA profile.**

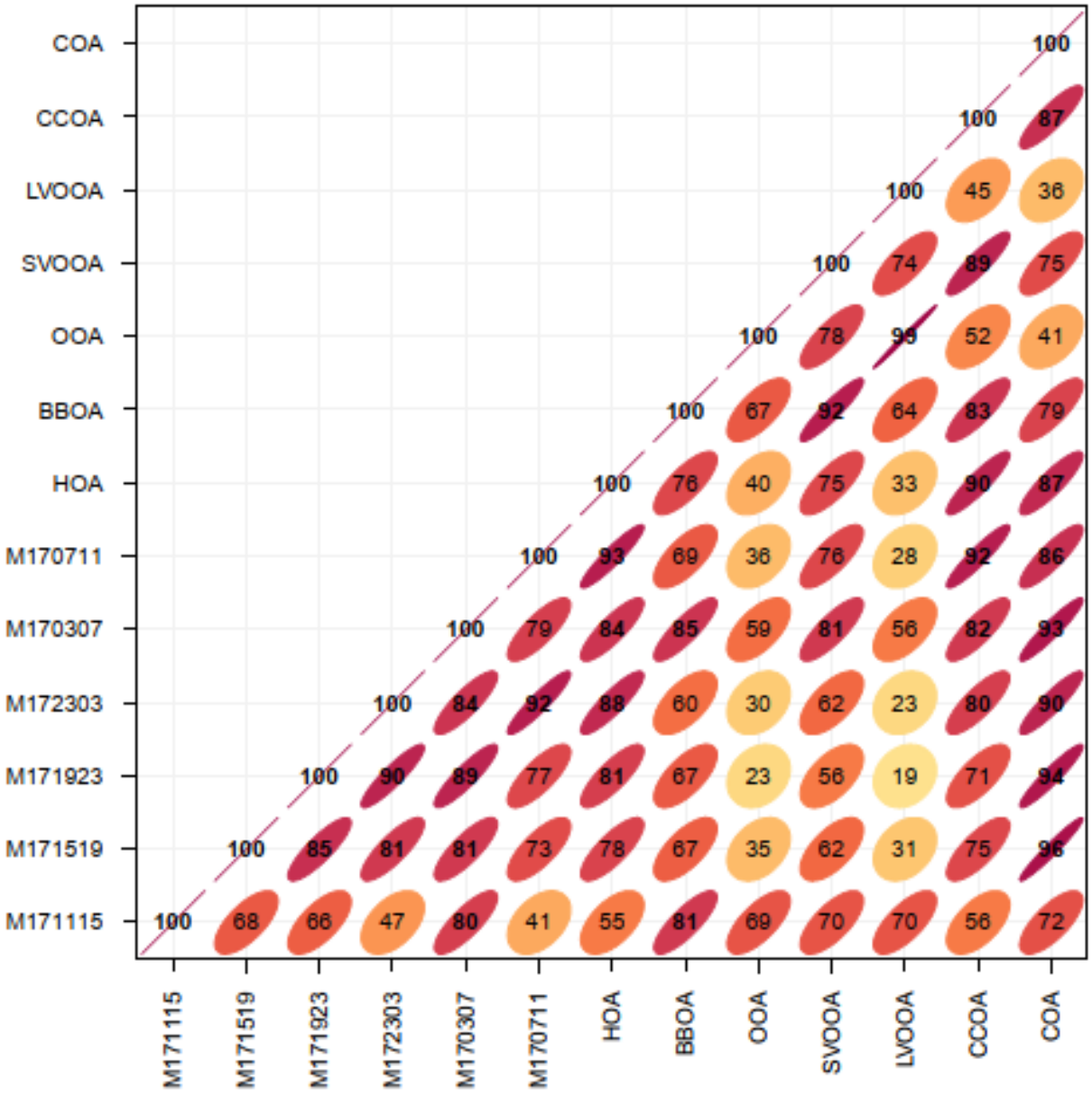

Figure S6 shows the mass spectral comparison of the time-of-day PMF COA MS profiles for monsoon 2017. Time-of-day PMF COA MS is strongly correlated to reference COA profile.

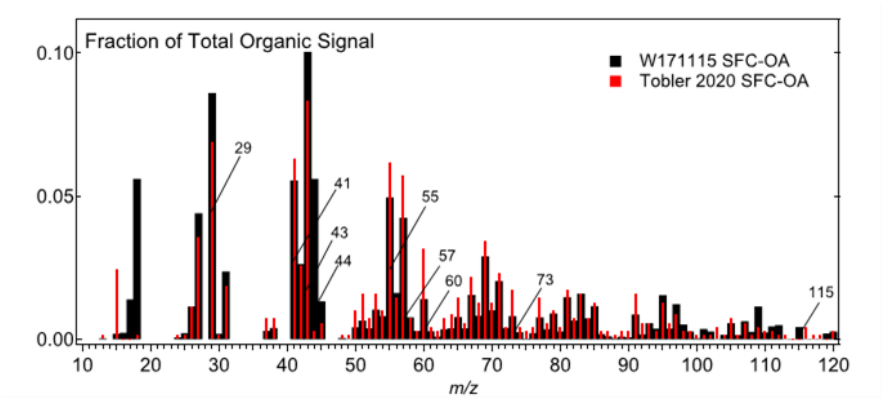

Figure S7 shows the mass spectrum of time-of-day PMF primary OA factor W171115 SFC-OA at winter midday in 2017 and the SFC-OA profile from the work of Tobler and co-workers (2020). W171115 SFC-OA MS shows strong similarities to the SFC-OA profile from literature, except at *m/z* 44.

135

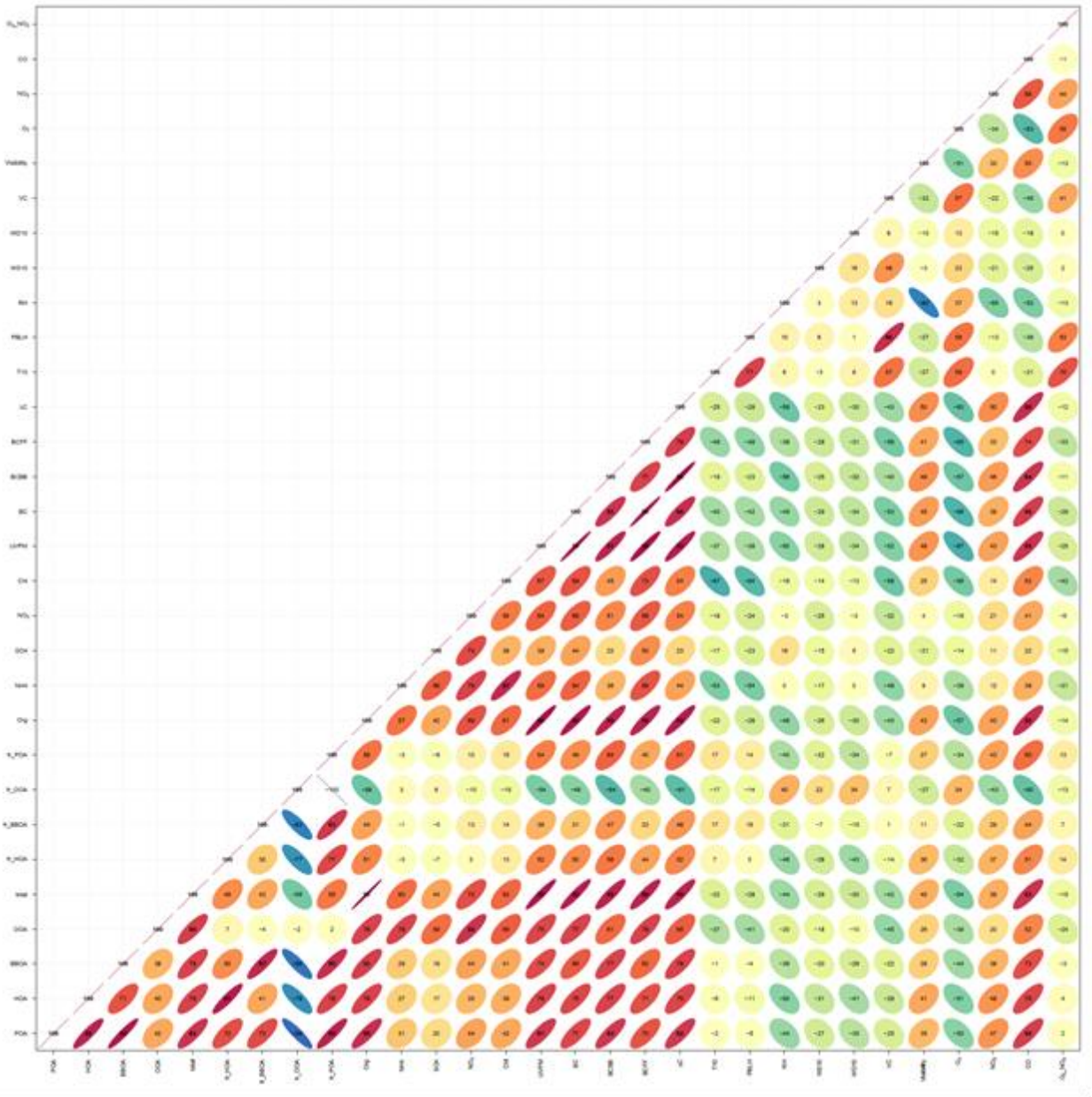

Figure S8 shows the time series correlations of the time-of-day PMF factors' TS and their fractions' TS with external tracers for the season of winter 2017 (for expanded figure, see Supplementary File-FigS8).

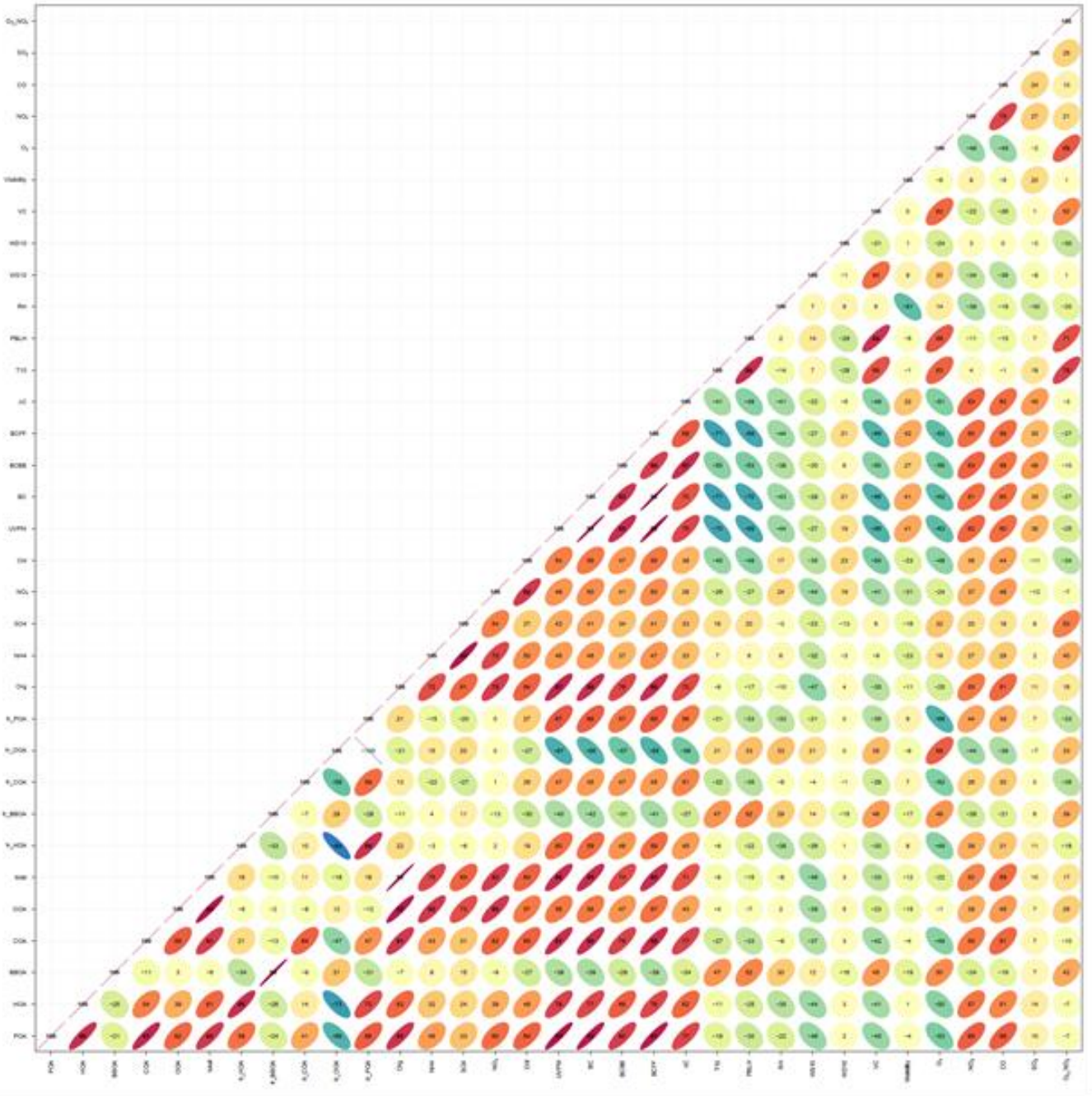

Figure S9 shows the time series correlations of the time-of-day PMF factors' TS and their fractions' TS with external tracers for the season of monsoon 2017 (for expanded figure, see Supplementary File-FigS9).

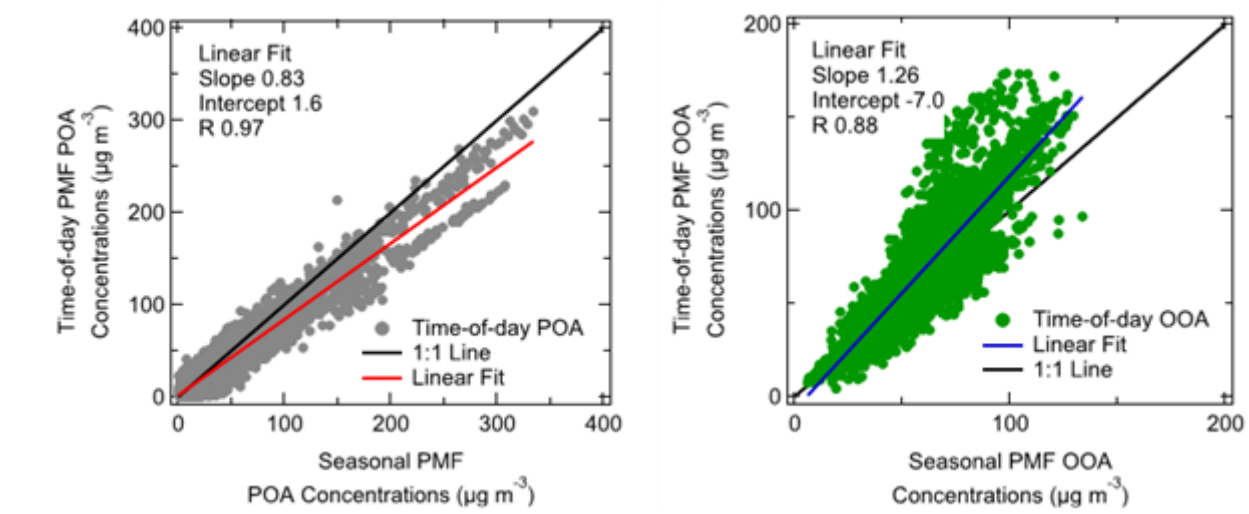

Figure S10 shows the comparison of time-of-day PMF and seasonal PMF- based factor concentrations (μg m^{-3}) for (a) the POA factor and (b) the OOA factor in winter 2017. The Pearson R coefficient indicates excellent linear correlations between the two analyses in all subplots. Based on the slope of the time series correlations, the time-of-day PMF estimates 17% less POA and about 26% more OOA than seasonal PMF in winter 2017.

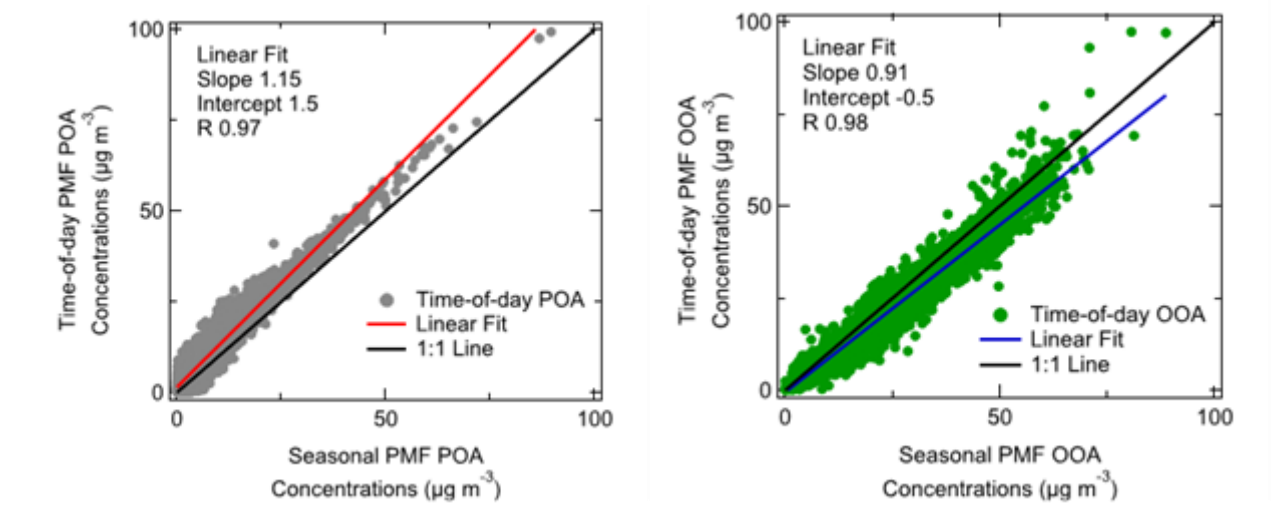

Figure S11 shows the comparison of time-of-day PMF and seasonal PMF- based factor concentrations (μg m^{-3}) for (a) the POA factor and (b) the OOA factor in monsoon 2017. The Pearson R coefficient indicates excellent linear correlations between the two analyses in all subplots. Based on the slope of the time series correlations, the time-of-day PMF estimates 26% more POA and about 9% less OOA than seasonal PMF in monsoon 2017.

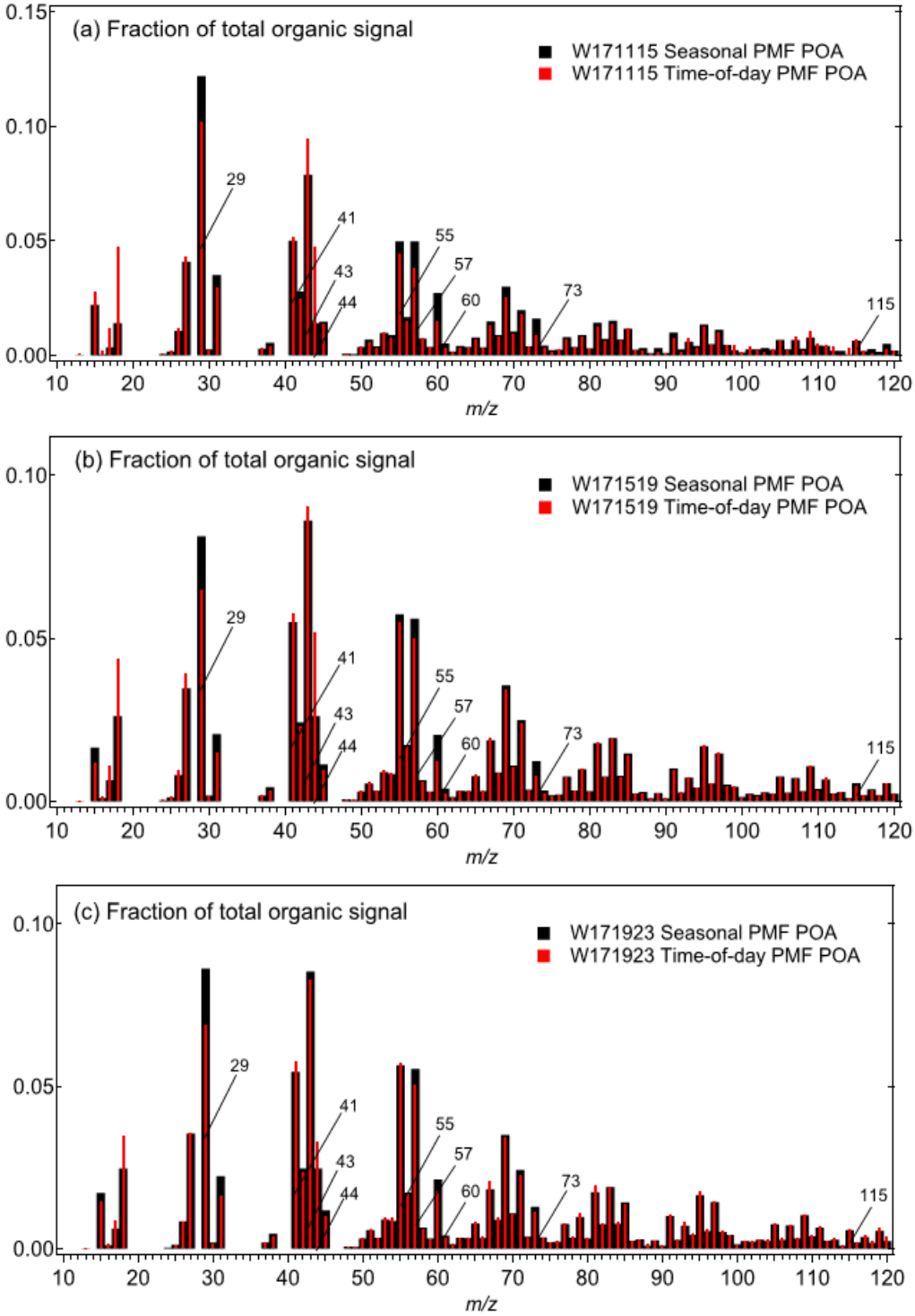

Figure S12 shows mass spectrum of seasonal and time-of-day PMF-based primary organic aerosol (POA) factor MS for the periods: (a) W171115, (b) W171519, (c) W171923, (d) W172303, (e) W170307, and (f) W170711 in winter 2017.

Figure S12 (continued)

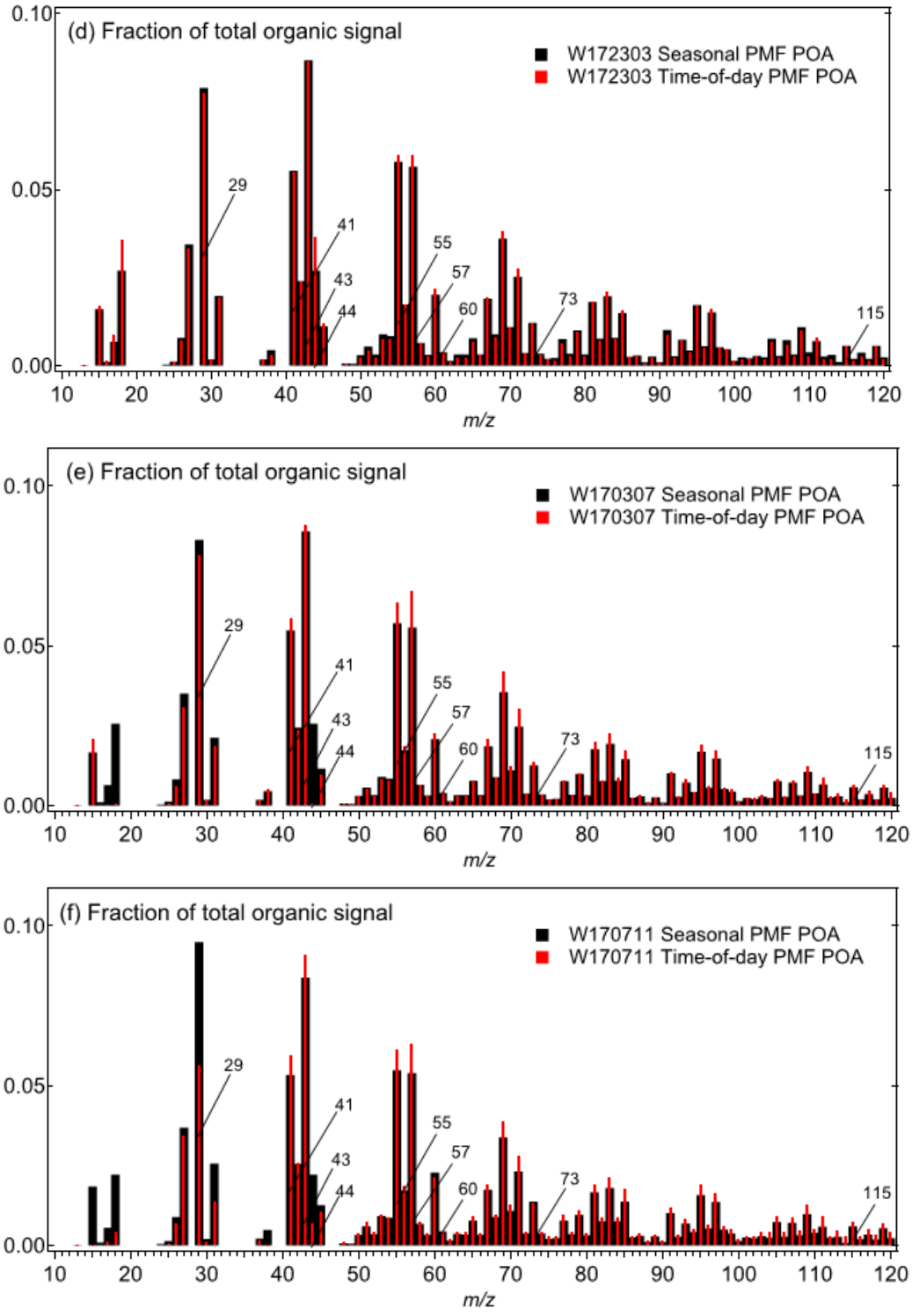

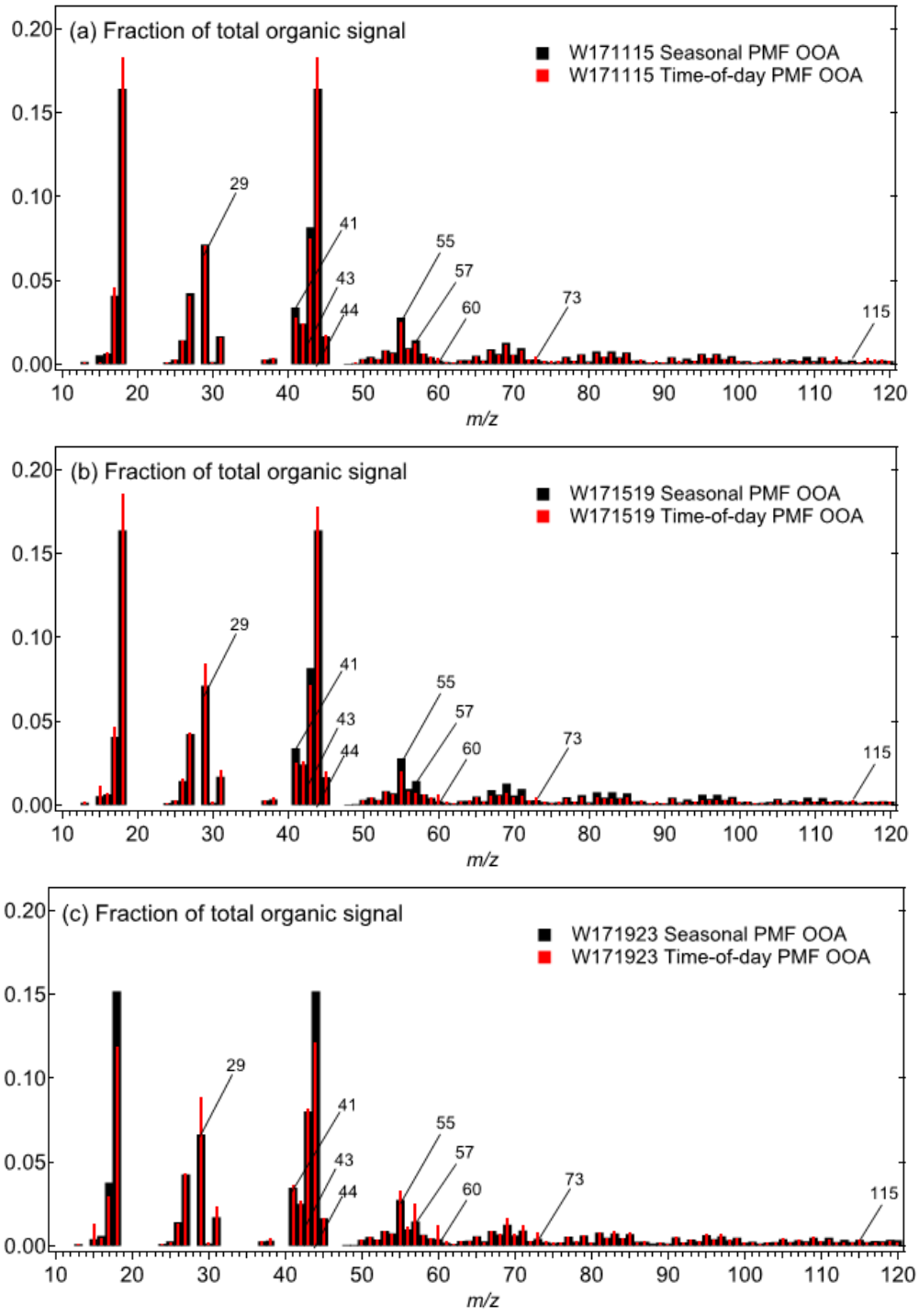

Figure S13 shows mass spectrum of seasonal and time-of-day PMF-based oxidized organic aerosol (OOA) factor MS for the periods: (a) W171115, (b) W171519, (c) W171923, (d) W172303, (e) W170307, and (f) W170711 in winter 2017.

Figure S13 (continued)

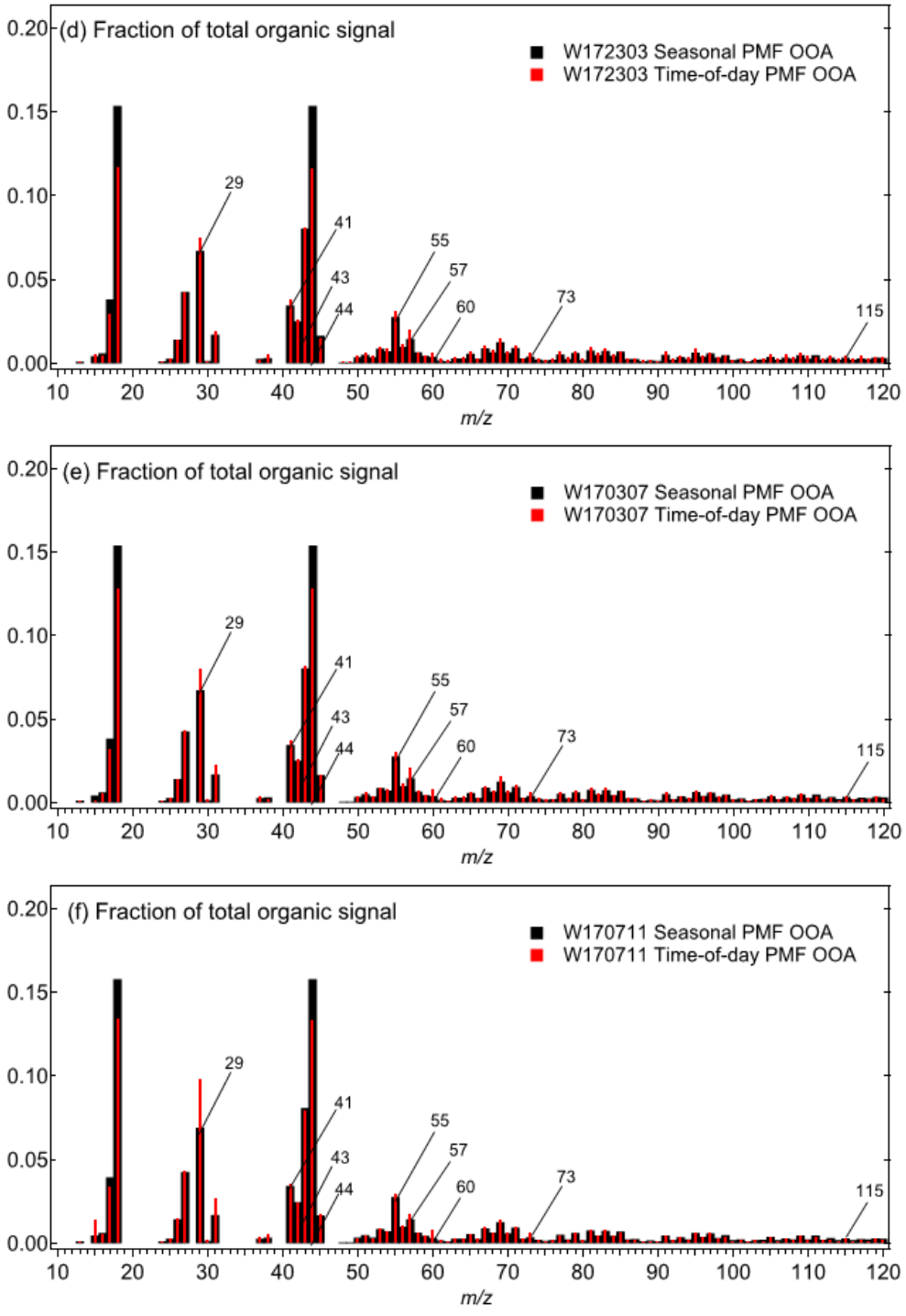

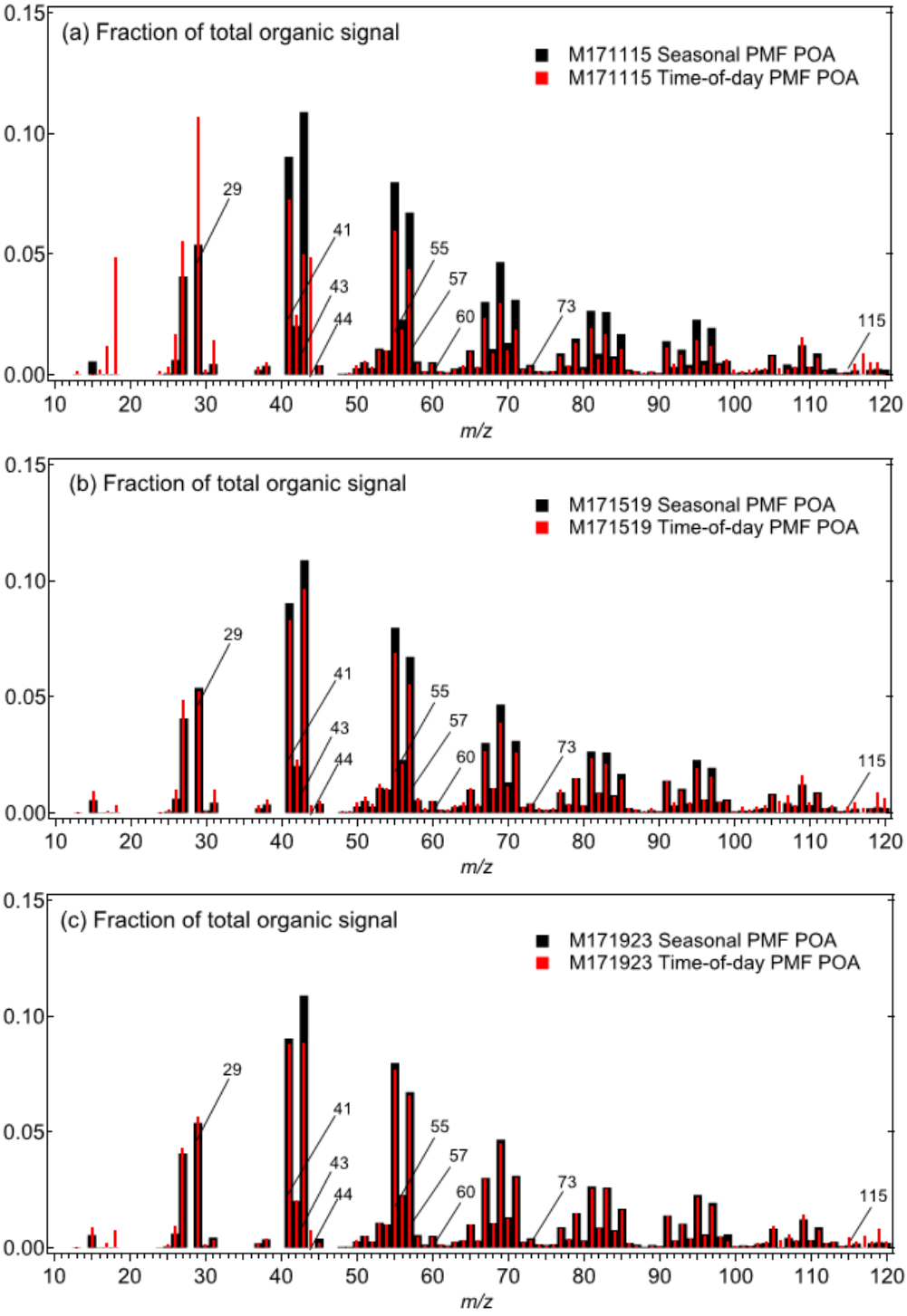

Figure S14 shows mass spectrum of seasonal and time-of-day PMF-based primary organic aerosol (POA) factor MS for the periods: (a) M171923, (b) M172303, (c) M170307, (d) M170711, (e) M171115, and (f) M171519 in monsoon 2017.

Figure S14 (continued)

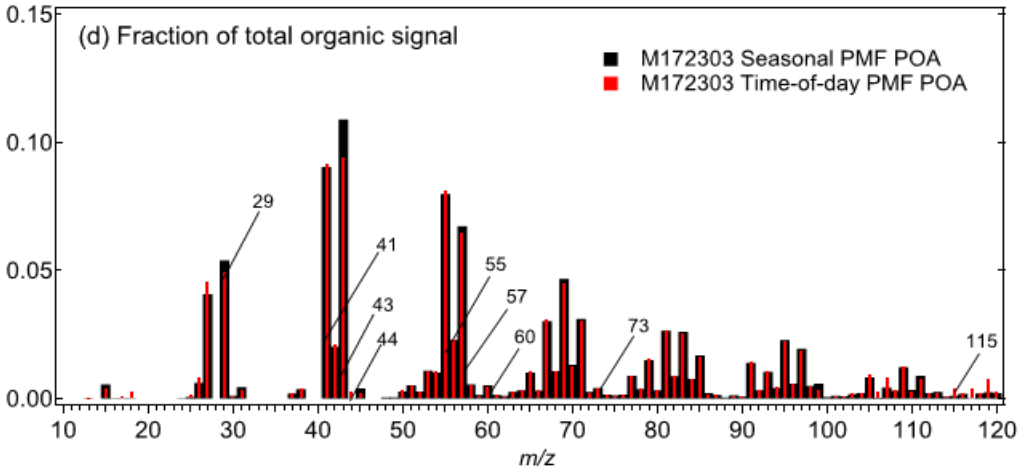

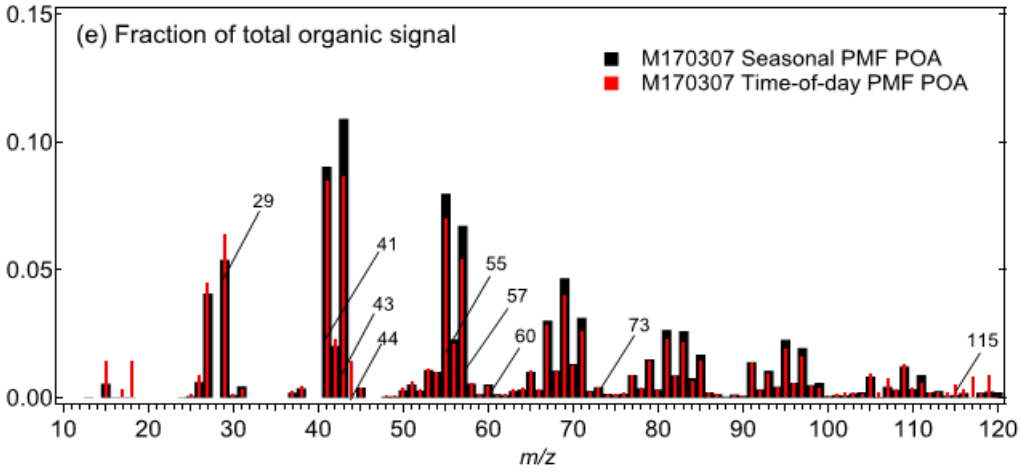

180

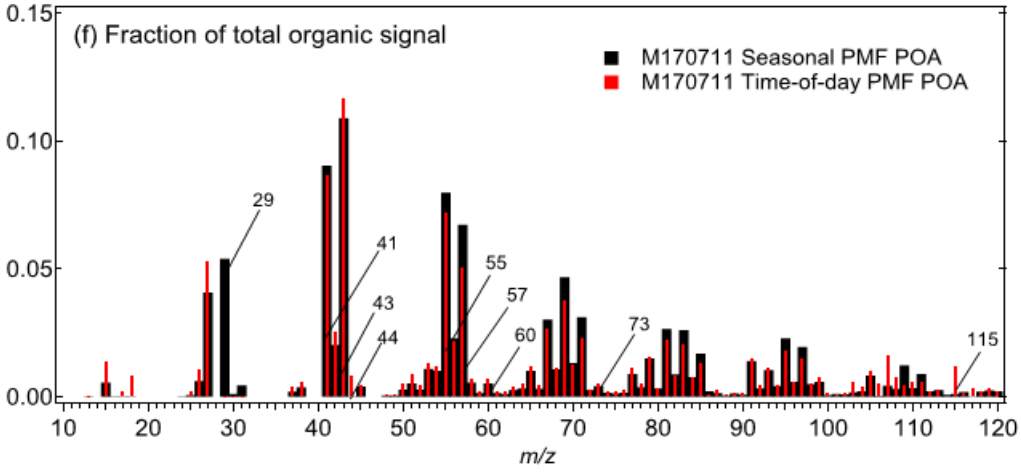

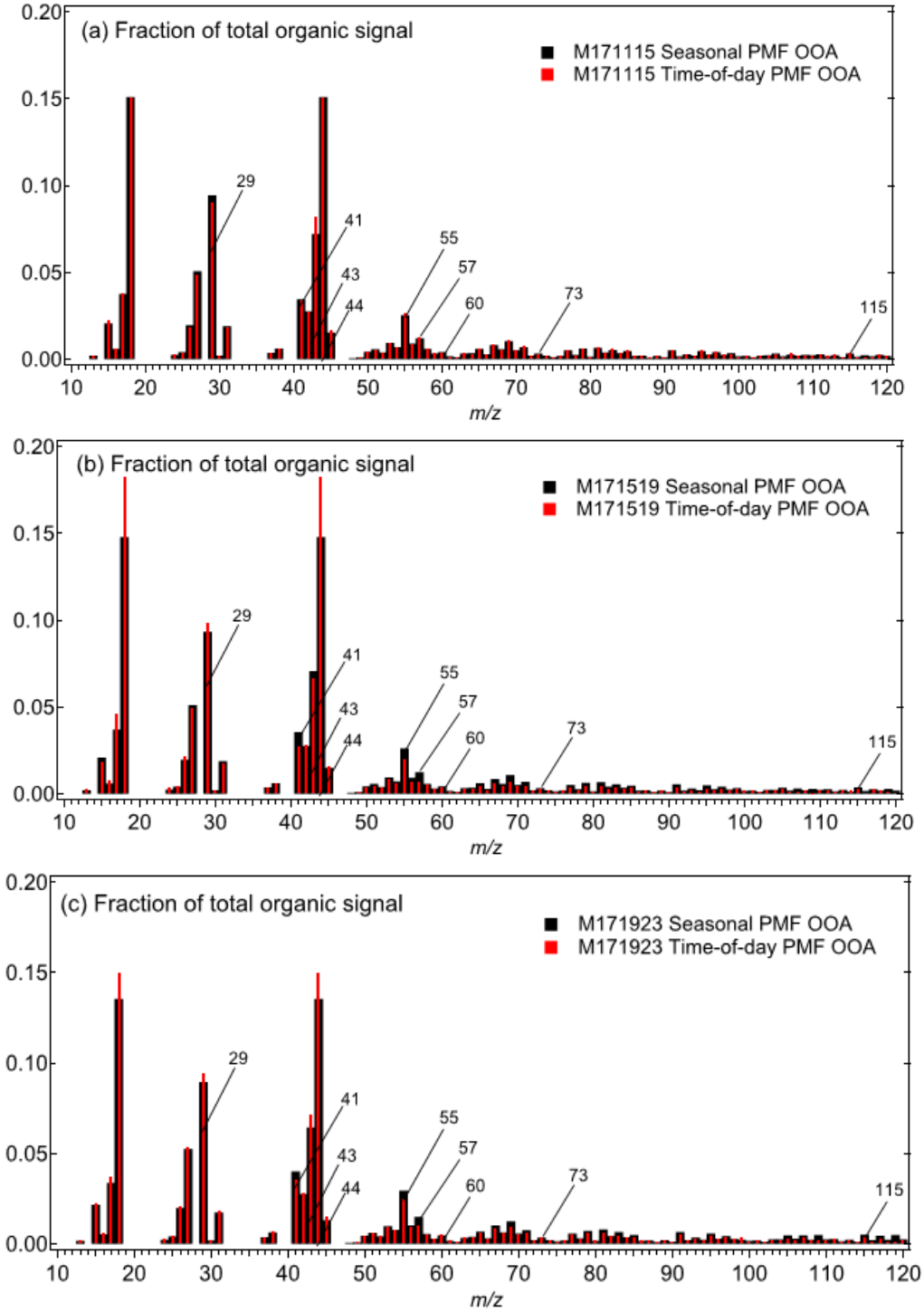

185 **Figure S15 shows mass spectrum of seasonal and time-of-day PMF-based oxidized organic aerosol (OOA) factor MS for the periods: (a) M171923, (b) M172303, (c) M170307, (d) M170711, (e) M171115, and (f) M171519 in monsoon 2017.**

Figure S15 (continued)

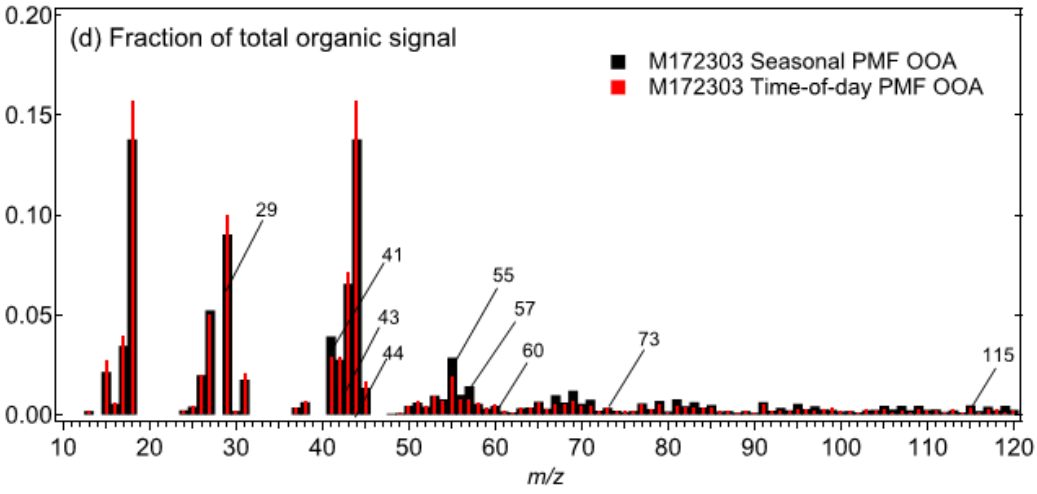

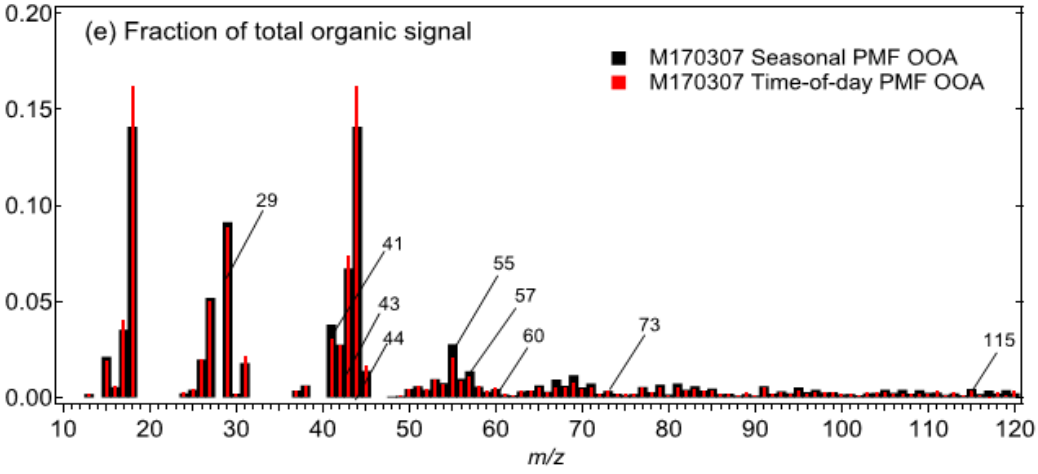

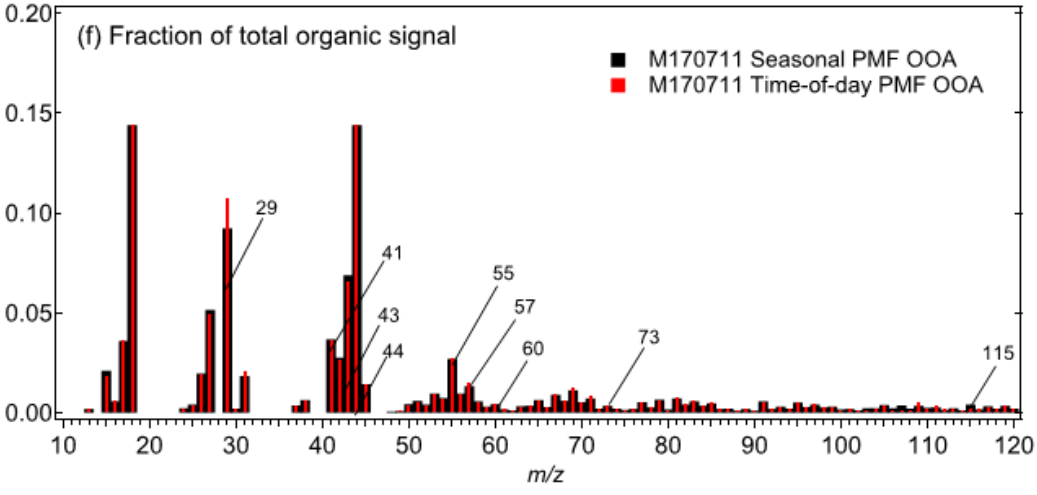

190

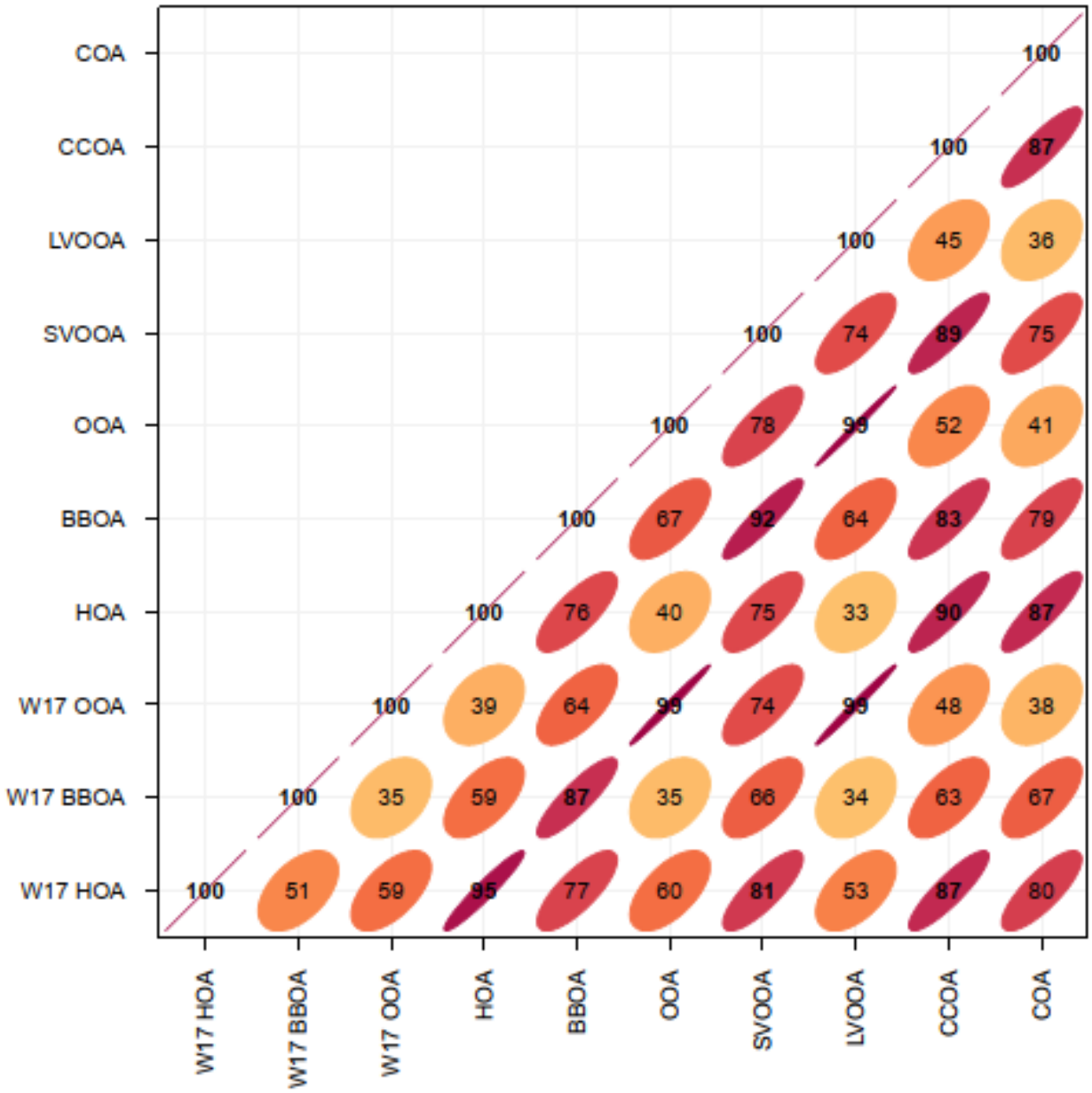

Figure S16 shows the mass spectral comparison of the seasonal PMF MS profiles with reference profiles for winter 2017. Each MS profile is correlated strongly to at least one reference profile.

195

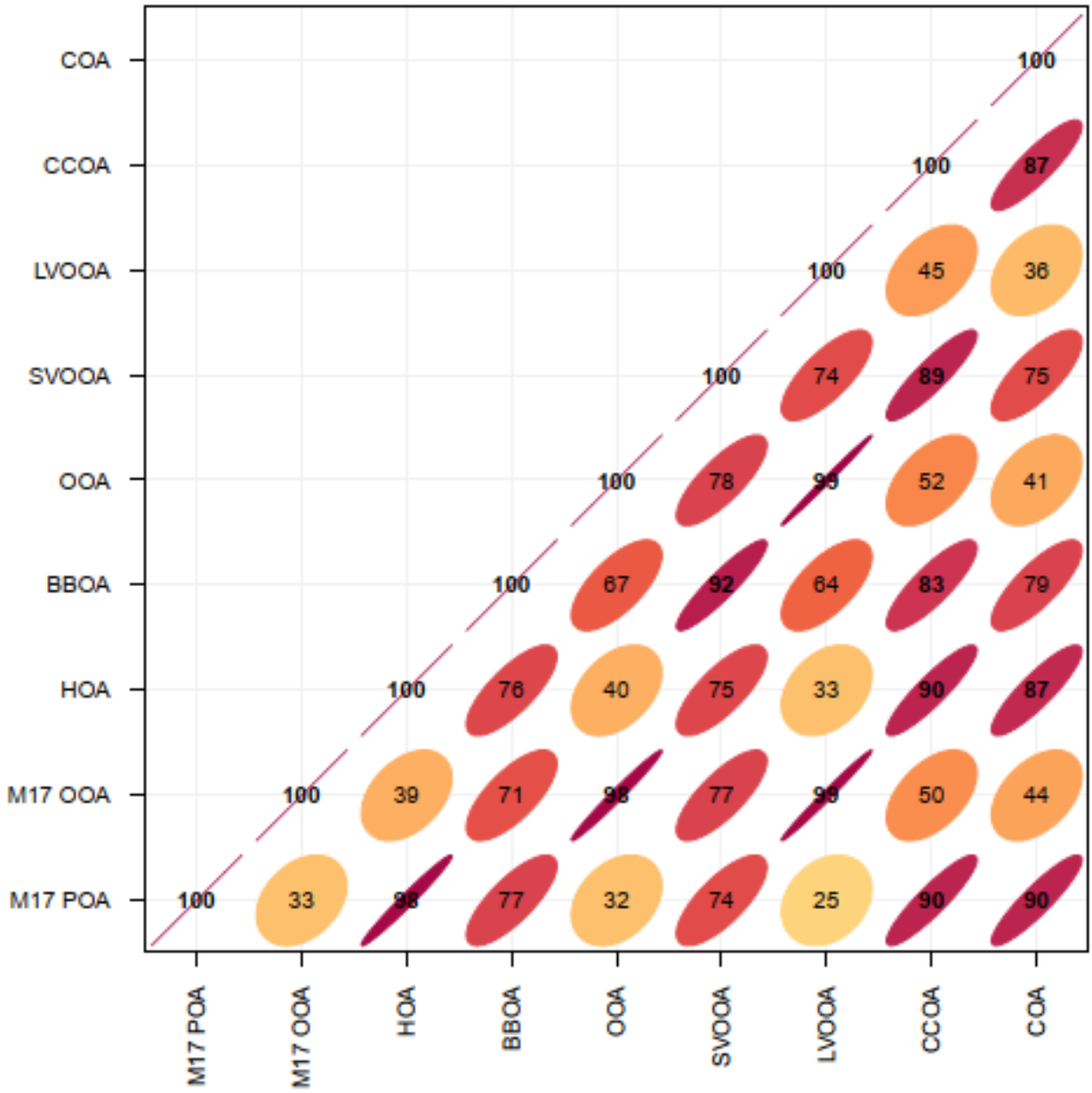

Figure S17 shows the mass spectral comparison of the seasonal PMF MS profiles with reference profiles for monsoon 2017. Each MS profile is correlated strongly to at least one reference profile.

200

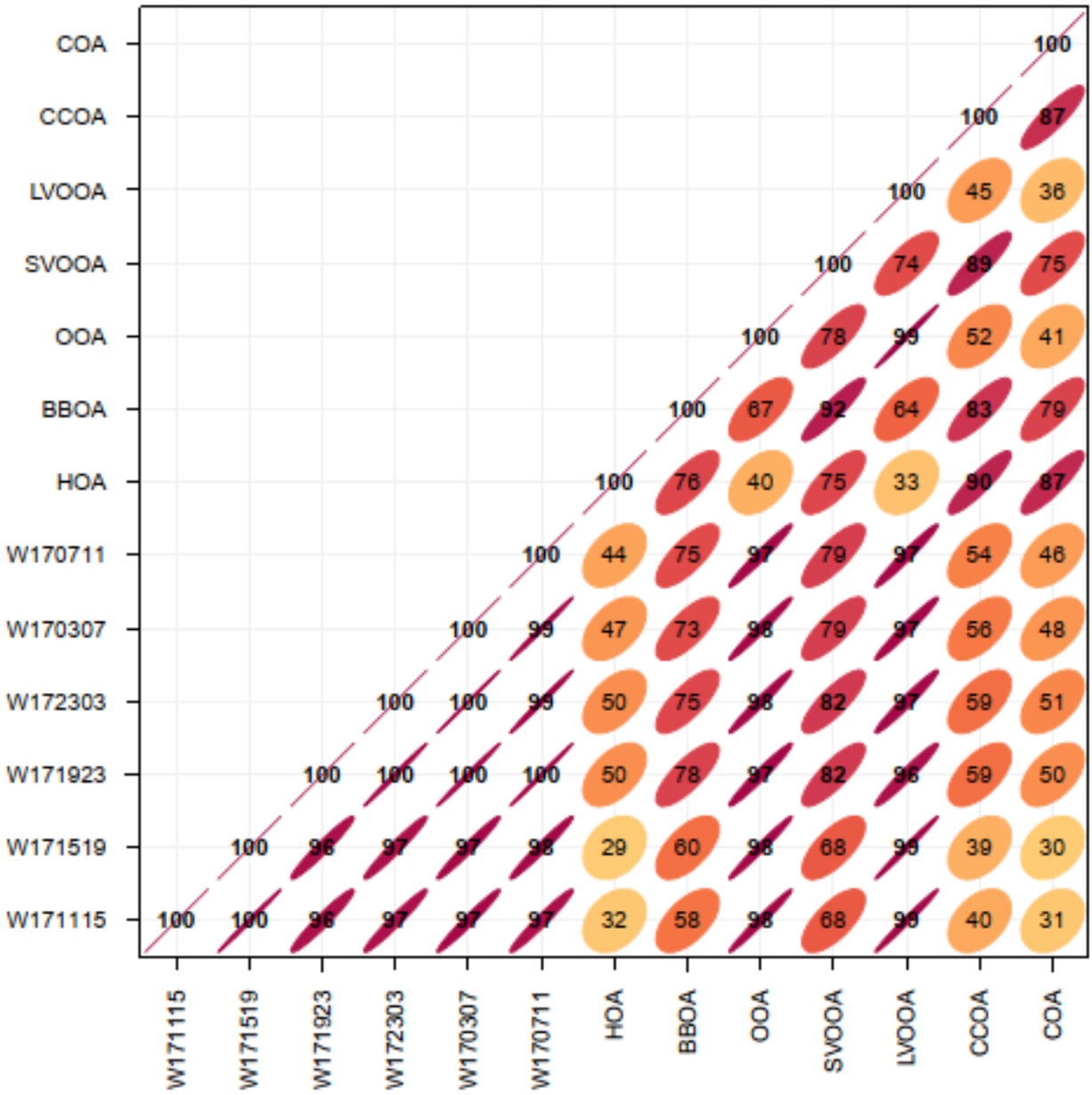

Figure S18 shows the mass spectral comparison of the time-of-day PMF OOA MS profiles with reference profiles for winter 2017. Each MS profile is correlated strongly to the reference OOA and LVOOA profiles.

205

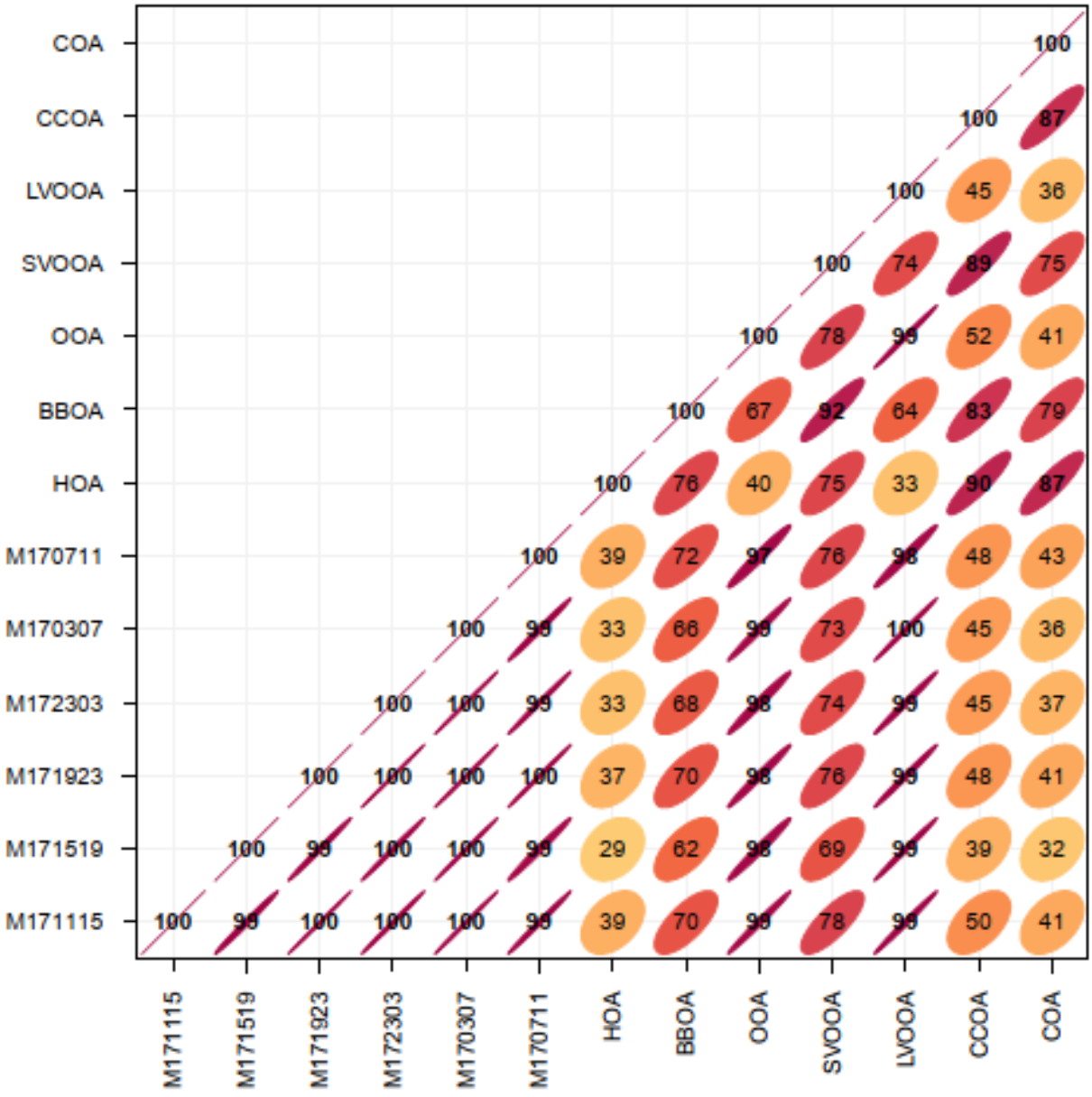

Figure S19 shows the mass spectral comparison of the time-of-day PMF OOA MS profiles with reference profiles for monsoon 2017. Each MS profile is correlated strongly to the reference OOA and LVOOA profiles.

S3 Application of the hybrid MLR-PMF approach

We applied the hybrid MLR-PMF approach on PMF primary factor MS for the 12 time-of-day windows. The hybrid MLR-PMF approach is applied only to separate POA factors into HOA, BBOA, and COA contributions. For application of this approach, we use reference MS profiles and MS profiles of known factors from the same period and their binary combinations as six starting points (three pure factors, three binary combinations of two factors at a time) to fit a multilinear regression to one primary factor MS at a time. At this first step, we minimize the error term in an iterative technique based on the Excel GRG Nonlinear Solver. The error term is based on a combination of a linear term (absolute error in matching overall MS) and a squared term (sum of fractional contributions of different primary components to overall TS in equalling unity). In this study, we have eight periods where PMF extracted two primary factors (two of HOA, BBOA, and COA). For consistency, we test this technique on those periods. Since PMF is typically expected to not resolve less than 5% OA as a factor, we also report mixing estimates based on MLR-PMF using the amount of mixing as a percent of total OA in a period. We call this mixing "Estimated mixing in PMF" (Tables S27–S28). The errors, obtained at step one, are generally comparable or even larger than the contributions of the smaller of the mixed factor components. Thus, the application of step one of the MLR-PMF approach results in large errors. We use this first step to narrow down to the one possibility among the six combinations that gives the lowest error. Next, we add a second layer to the analysis to reduce the error further. Starting at the possible solution above, we allow one of the three factor profiles to move freely. Our hypothesis is that such freedom will allow the solution to converge to a more optimal solution. Our observations line up with this hypothesis; the error lowers dramatically (Tables S27–S28). We only select solutions with low errors and feasible MS profiles.

Table S27 Errors obtained in fits using the MLR-PMF approach for winter 2017

Period/Factor	Errors at Step 1	Final Error	Estimated mixing in PMF (%OA)	Free profile
W171115 SFC-OA	1.31	0.05	Not Applicable[a]	BBOA
W171115 BBOA	0.98	0.01	0	BBOA
W171519 HOA	0.77	0.04	0	BBOA
W171519 BBOA	0.40	<0.01	1.9	BBOA
W171923 HOA	1.82	0.09	0.4	HOA
W171923 BBOA	2.22	<0.01	3.7	BBOA
W172303 HOA	1.96	<0.01	5.0	HOA
W172303 BBOA	2.63	<0.01	2.4	BBOA
W170307 POA	2.46	0.07	Not Applicable[b]	BBOA
W170711 HOA	0.89	0.19	0.5	BBOA
W170711 BBOA	1.29	0.07	3.6	BBOA

[a]SFC-OA was assumed to contain HOA, BBOA, and COA [b]This period extracted only one POA factor

Table S28 Errors obtained in fits using the MLR-PMF approach for monsoon 2017

Period/Factor	Error at Step 1	Final Error	Estimated mixing in PMF (%OA)	Free profile
M171115 POA	0.28	0.02	Not applicable[a]	COA
M171519 HOA	0.06	<0.01	3.8	HOA
M171519 COA	0.23	0.06	1.7	COA
M171923 HOA	0.42	<0.01	0	HOA
M171923 COA	0.48	<0.01	2.5	COA
M172303 HOA	0.16	<0.01	0.6	HOA
M172303 COA	0.24	<0.01	0	COA
M170307 HOA	0.18	<0.01	0.4	HOA
M170307 COA	0.21	0.03	2.4	COA
M170711 POA	0.19	<0.01	Not applicable[a]	COA

[a]This period extracted only one POA factor

S4 Application of the Volatility Basis Set

Combining data from laboratory studies and field campaigns in Paris, Greece and Finokalia, Pandis and co-workers have shown that the 1-D volatility basis set (VBS, Donahue et al., 2006) obtained for different source apportionment factors (based on the external mixture assumption) are reasonably representative of the volatility of the actual mixed aerosol system and are similar once normalized for concentrations (Karnezi et al., 2018). Detailed comparisons of VBS across studies are subject of a separate publication (Dinh et al., in preparation). PMF factor concentrations in Delhi can exceed 10 μg m^{-3}, as shown in Tables 1 and 2. In the absence of volatility data for Delhi, we use the Mexico City VBS for HOA and BBOA due to the availability of data from the volatility bin Ci* (298 K) equal to 100 μg m^{-3} (Cappa and Jimenez, 2010). The Athens VBS is the only study that separated all three primary factors—HOA, BBOA, and COA (Louvaris et al., 2017). We use estimates based on the Athens study, even though the highest volatility bin Ci* (298 K) is equal to 10 μg m^{-3}. We assume constant gas plus particle phase fractions corresponding to volatility bins ($\log_{10}$C* (in μg m^{-3})) from 10^{-7} to 10^{2} for the Mexico VBS and 10^{-7} to 10^{1} for the Athens study. We use PMF-based Delhi particle phase data to estimate total concentrations (gas plus particle phase) that, under conditions of equilibrium partitioning, generate measured concentrations in the particle phase. We run the above procedure on time-of-day PMF-based seasonally representative diurnal averages for the different primary factors. In the first round of runs, diurnal data for winter and monsoon of 2017 is input together with actual temperature to generate equilibrium concentrations of gas-phase organics. We refer to the output at this step as "source" concentrations. In the second

round, to estimate maximum PM formation potential relative to the sources of HOA and COA in monsoon 2017, diurnal "source" concentration averages of HOA and BBOA for winter 2017 are applied to monsoon—the goal being to allow repartitioning for achieving equilibrium. We call these PMF factors "winter-to-monsoon" HOA and BBOA. These "source" concentrations are corrected for VC effects using linear corrections. The limitation of this approach is that using linear corrections for ventilation coefficient might be overcompensating its effect. In the third round, the "source" concentrations for HOA and COA in monsoon 2017, corrected for VC effects, are run with the temperature of winter 2017. We call these PMF factors "monsoon-to-winter" HOA and COA.

S5 References

1. Dinh, A., Bhandari, S., Habib, G., Apte, J., Ruiz, L. H.: Effect of gas-particle partitioning on source apportionment of ambient mass spectrometry data (in preparation), 2022.
2. Donahue, N. M., Robinson, A. L., Stanier, C. O., and Pandis, S. N.: Coupled partitioning, dilution, and chemical aging of semivolatile organics, Environmental Science & Technology, 40, 2635–2643, URL https://doi.org/10.1021/es052297c, 2006.
3. Gani, S., Bhandari, S., Seraj, S., Wang, D. S., Patel, K., Soni, P., Arub, Z., Habib, G., Hildebrandt Ruiz, L., and Apte, J.: Submicron aerosol composition in the world's most polluted megacity: The Delhi Aerosol Supersite study, Atmospheric Chemistry and Physics, 19, 6843–6859, URL https://doi.org/10.5194/acp-19-6843-2019, 2019.
4. Hu, W., Hu, M., Hu, W., Jimenez, J. L., Yuan, B., Chen, W., Wang, M., Wu, Y., Chen, C., Wang, Z., Peng, J., Zeng, L., and Shao, M.: Chemical composition, sources, and aging process of submicron aerosols in Beijing: contrast between summer and winter, Journal of Geophysical Research, 121, 1955–1977, URL https://doi.org/10.1002/2015JD024020, 2016.
5. Karnezi, E., Louvaris, E., Kostenidou, E., Florou, K., Cain, K., and Pandis, S.: Discrepancies between the volatility distributions of OA in the ambient atmosphere and the laboratory, International Aerosol Conference, URL http://aaarabstracts.com/2018IAC/viewabstract.php?pid=870, 2018.
6. Louvaris, E. E., Florou, K., Karnezi, E., Papanastasiou, D. K., Gkatzelis, G. I., and Pandis, S. N.: Volatility of source apportioned wintertime organic aerosol in the city of Athens, Atmospheric Environment, 158, 138–147, URL https://doi.org/10.1016/j.atmosenv.2017.03.042, 2017.
7. Ng, N. L., Canagaratna, M. R., Jimenez, J. L., Zhang, Q., Ulbrich, I. M., and Worsnop, D. R.: Realtime methods for estimating organic component mass concentrations from aerosol mass spectrometer data, Environmental Science and Technology, 45, 910–916, URL https://pubs.acs.org/doi/abs/10.1021/es102951k, 2011a.
8. Ng, N. L., Herndon, S. C., Trimborn, A., Canagaratna, M. R., Croteau, P. L., Onasch, T. B., Sueper, D., Worsnop, D. R., Zhang, Q., Sun, Y. L., and Jayne, J. T.: An Aerosol Chemical Speciation Monitor (ACSM) for routine monitoring of the composition and mass concentrations of ambient aerosol, Aerosol Science and Technology, 45, 780–794,

URL http://www.tandfonline.com/doi/abs/10.1080/02786826.2011.560211, 2011b.

9. ResearchGate, https://www.researchgate.net/post/Has-anybody-observed-strange-discontinuities-in-ERA5s-diurnal-cycle-of-temperature-precipitation-etc, 2021.
10. Tobler, A., Bhattu, D., Canonaco, F., Lalchandani, V., Shukla, A., Thamban, N. M., Mishra, S., Srivastava, A. K., Bisht, D. S., Tiwari, S., Singh, S., Mocnik, G., Baltensperger, U., Tripathi, S. N., Slowik, J. G., and Prévôt, A. S.: Chemical characterization of PM2.5 and source apportionment of organic aerosol in New Delhi, India, Science of the Total Environment, 745, 140924, URL https://doi.org/10.1016/j.scitotenv.2020.140924, 2020.